POLR3-Related Leukodystrophy: Generation of isogenic controls from patient-derived induced pluripotent stem cells and exploration of disease pathogenesis using neural progenitor cells

Neeti Jain

Integrated Program in Neuroscience

Department of Neurology and Neurosurgery

McGill University, Montreal

June 2023

A thesis submitted to McGill University in partial fulfillment of the requirements of the degree of Master of Science

Table of Contents

Abstract

Hypomyelinating leukodystrophies are a group of rare, inherited white matter disorders characterized by abnormal myelin deposition during development.[1,2] RNA polymerase III-related hypomyelinating leukodystrophy (POLR3-HLD) is caused by biallelic pathogenic variants in genes encoding the RNA polymerase III (Pol III) subunits.[3–7] Pol III is responsible for the transcription of small non-coding RNAs with important roles in gene expression and protein synthesis.[8] POLR3-HLD has a wide phenotypic spectrum and the underlying pathophysiology of how biallelic pathogenic variants in the genes encoding Pol III subunits leads to the phenotypes seen has yet to be elucidated.[9]

Due to the small sample size inherently present in rare disease research, accurate cellular models of disease must be developed to perform robust *in vitro* experiments to understand these disorders at a cellular and molecular level. This project aimed to generate accurate controls, such as isogenic controls developed through CRISPR/Cas9 genome engineering using patient-derived induced pluripotent stem cells (iPSCs), to facilitate further studies on the disease pathogenesis of POLR3-HLD.

Some patients with the severe phenotype harbor a specific genotype with compound heterozygous biallelic pathogenic variants in *POLR3A*, which includes variants causing the c.1771-7C>G intronic splicing variant and a premature stop codon.[9] While POLR3-HLD typically presents with frank hypomyelination, prior neuropathological analysis on patients with a severe presentation of POLR3-HLD showed predominant neuronal abnormalities.[9] Therefore, we hypothesize that the c.1771-7C>G intronic splicing variant leads to decreased levels of Pol III transcripts in patient cells as they are differentiated into neural progenitor cells, suggesting that is what contributes to the abnormal phenotype seen in patients with severe POLR3-HLD.[9]

This project aims to better understand the relationship between the genotype and phenotype of patients with POLR3-HLD and examine potential differences in Pol III function in various severe POLR3-HLD patient cell types. To evaluate pathophysiological mechanisms underlying the abnormal neuronal defects seen in this cohort of patients, patient-derived iPSCs were used to generate cortical neural progenitor cells (NPCs). Pol III target levels were then evaluated with RNA from iPSCs, NPCs, and fibroblasts from patient and control cell lines. Overall, it was observed that more Pol III target levels were significantly affected in patient fibroblasts and iPSCs, as compared to NPCs. It was also seen that tRNA levels were significantly affected in patient iPSCs as compared to controls, which was not seen in fibroblasts or NPCs. Furthermore, Patient 4 fibroblasts and iPSCs had the most Pol III targets significantly altered, as compared to Patient 5 and Patient 6, while Patient 6 NPCs had the most Pol III targets that were significantly decreased, as compared to Patient 4 and Patient 5.

The methodology developed here will help further study the disease pathogenesis by better understanding how to develop isogenic controls using patient-derived iPSCs and highlighting the importance of measuring Pol III transcript levels in various cell types. It is hoped that this evaluation will open the door for the development of potential therapeutics for this devastating neurodegenerative disease.

Résumé

Les leucodystrophies hypomyélinisantes sont un groupe de maladies rares et héréditaires de la substance blanche, caractérisées par un dépôt anormal de myéline pendant le développement. La leucodystrophie hypomyélinisante liée à l'ARN polymérase III (POLR3-HLD) est causée par des variants pathogènes bialléliques dans les gènes codant les sous-unités de l'ARN polymérase III (Pol III). Pol III est responsable de la transcription de petits ARN non codants jouant un rôle essentiel dans l'expression génique et la synthèse des protéines. POLR3-HLD présente un large spectre phénotypique et la physiopathologie sous-jacente de la manière dont les variants pathogènes bialléliques dans les gènes codant les sous-unités de Pol III conduisent aux phénotypes observés reste à élucider.

En raison des petites tailles d'échantillons intrinsèquement présentent pour la recherche sur les maladies rares, il est nécessaire de développer des modèles cellulaires précis de la maladie pour réaliser des expériences *in vitro* robustes afin de comprendre ces maladies au niveau cellulaire et moléculaire. Ce projet visait à générer des contrôles précis, tels que des contrôles isogéniques développés grâce à l'ingénierie du génome CRISPR/Cas9 avec des cellules souches pluripotentes induites (iPSC) dérivées de patients, afin de mieux faciliter les études visant à étudier la physiopathologie de la leucodystrophie liée à l'ARN polymérase III.

Certains patients présentant un phénotype sévère ont un génotype spécifique avec des variants pathogènes bialléliques hétérozygotes dans POLR3A, ce qui inclut des variants entraînant la variation d'épissage intronique c.1771-7C>G et un codon stop prématuré. Alors que POLR3-HLD se manifeste généralement par une hypomyélinisation nette, une analyse neuropathologique antérieure sur des patients présentant une forme sévère de POLR3-HLD a révélé des anomalies neuronales prédominantes. Par conséquent, nous émettons l'hypothèse que la variation d'épissage

intronique c.1771-7C>G conduit à une diminution des niveaux de transcrits de Pol III dans les cellules des patients lorsqu'elles se différencient en cellules progénitrices neurales, suggérant que cela contribue au phénotype anormal observé chez les patients atteints de POLR3-HLD sévère.

Ce projet vise à mieux comprendre la relation entre le génotype et le phénotype des patients atteints de POLR3-HLD et à examiner les éventuelles différences de fonction de Pol III dans différents types cellulaires de patients atteints de POLR3-HLD sévère. Pour évaluer les mécanismes physiopathologiques sous-jacents aux défauts neuronaux anormaux observés dans cette cohorte de patients, iPSC dérivées de patients ont été utilisées pour générer des cellules progénitrices neurales corticales (NPC). Les niveaux cibles de Pol III ont ensuite été évalués à l'aide d'ARN provenant d'iPSC, de NPC et de fibroblastes de lignées cellulaires de patients et de contrôles. Dans l'ensemble, on a observé que les niveaux de cibles de Pol III étaient significativement affectés dans les fibroblastes et les iPSCs des patients, par rapport aux NPCs. On a également constaté que les niveaux de tRNA étaient significativement affectés dans les iPSCs des patients par rapport aux témoins, ce qui n'est pas observé dans les fibroblastes ou les NPCs. De plus, les fibroblastes et les iPSCs du Patient 4 présentaient le plus grand nombre de cibles de Pol III significativement altérées, par rapport aux Patients 5 et 6, tandis que les NPCs du Patient 6 présentaient le plus grand nombre de cibles de Pol III significativement diminuées, par rapport aux Patients 4 et 5.

La méthodologie développée ici aidera à approfondir l'étude de la pathogenèse de la maladie en comprenant mieux comment développer des contrôles isogéniques en utilisant des iPSC dérivées de patients, et en mettant en évidence l'importance de mesurer les niveaux de transcrits Pol III dans différents types de cellules. On espère que cette évaluation ouvrira la voie au développement de thérapies potentielles pour cette maladie neurodégénérative dévastatrice.

Acknowledgments

I would like to begin by expressing my deepest gratitude to my supervisor, Dr. Geneviève Bernard, for her support and guidance throughout this research project. Dr. Bernard's expertise, dedication, and mentorship have been invaluable in shaping the direction of this research project and myself as a researcher. This thesis has been a pivotal moment in my academic career and Dr. Bernard's kindness and commitment to excellence has aided me immensely. It is through the mentorship of a clinician-scientist such as Dr. Bernard, that I have been able to fully understand the meaning of hard-work, dedication, and compassion.

I would also like to take this time to thank the phenomenal MyeliNeuroGene Lab team for their support with this project and for their friendship. I would like to thank Dr. Stefanie Perrier and Alexandra Chapleau for introducing me to the world of iPSCs and CRISPR, and for being my first friends in Montreal. This thesis would not have been possible without their guidance and support and for that, I am forever grateful. I would also like to extend my gratitude to Julia Macintosh for being so kind and patient when assisting with RNA extractions and RT-qPCR. I will always be thankful for the support of Xiaoru Chem and Chia-Lun Wu, who were always there to support my project in any way they could. Laura Lentini, thank you for brightening up our weekly lunches and always being there to listen and provide advice, I am so thankful for our friendship. Lastly, I would like to thank Helia Toutounchi, Luan Tran, Mackenzie Michell-Robinson, Simon Fournier, Fatosh Emari and Adam Le for being amazing pillars of support.

I want to extend my appreciation to my three committee members, Dr. Thomas Durcan, Dr. Carl Ernst, and Dr. Timothy Kennedy, for their support and guidance throughout this master's project. Their expert advice during committee meetings and invaluable guidance through their research platform helped shape this masters project. Their challenging questions and honest advice

were what helped me realize which direction I wanted to take the project in and what key aspects to focus on. I would also like to acknowledge my IPN mentor, Dr. Xiaoqian Chai, for chairing the thesis seminar.

I also want to thank the IPN program at McGill, the Montreal Neurological Institute (especially the Early Drug Discovery Unit for providing me with support and guidance throughout their various protocols I used), the McGill University Health Center Research Institute (Child Health and Human Development Department), and the Desjardins Studentship and Fellowship award.

Lastly, appreciation is due for my wonderful family whose love and support has radiated from my home in Toronto. I would not be the person I am today without my parents (Neeraj and Sonal Jain), brother (Shikhar Jain), grandparents and extended family and family friends. Furthermore, I am grateful for many amazing friends in Montreal and in Toronto, who have done nothing but cheer me on since I started. Thank you to Alexis Chacon, Farseema Delgosha, Omid Mahboubi, Naga Thovinakere, Olivia Bizimungu, Ajeetpall Singh, Eleri McEachern and Shahd Fares. I am so thankful to receive so much unconditional love from so many amazing people. I acknowledge the privilege I have to be able to achieve what I did, and I hope to support other immigrant women of colour in neuroscience throughout my career.

Contributions

Neeti Jain wrote this thesis with assistance from Julia Macintosh, Alexandra Chapleau, and Dr. Geneviève Bernard. The abstract was translated to French with the help of Simon Fournier. Neeti Jain has conducted all the experiments in this thesis, with assistance from members of the lab. Dr. Stefanie Perrier and Alexandra Chapleau aided in learning cell culture techniques for iPSCs and NPCs, and the CRISPR/Cas9 genome engineering process. Julia Macintosh assisted in fibroblast culturing and experiments related to RT-qPCR. Dr. Chia-Lun Wu assisted in immunocytochemistry experiments.

List of Figures and Tables

List of Abbreviations

POLR3-HLD	RNA polymerase III-related hypomyelinating leukodystrophy
Pol III	RNA polymerase III
iPSC	Induced Pluripotent Stem Cell
NPC	Neural Progenitor Cell
CNS	Central Nervous System
MRI	Magnetic Resonance Imaging
LO	Leukodystrophy with Oligodontia
ADDH	Ataxia, Delayed Dentition, and Hypomyelination
HCAHC	Hypomyelination with Cerebellar Atrophy and Hypoplasia of the Corpus Callosum
TACH	Tremor-Ataxia with Central Hypomyelination
WRS	Wiedemann-Rautenstrauch Syndrome
Pol I	RNA Polymerase I
rRNA	Ribosomal RNA
Pol II	RNA Polymerase II
ncRNA	Non-coding RNA
tRNA	Transfer RNA
SINE	Short Interspersed Element
PBMC	Peripheral Blood Mononuclear Cells
TGF-β	Transforming Growth Factor Beta
BMP	Bone Morphogenic Protein
DMH1	Dorsomorphin Homolog 1
ALK	Activin Receptor-Like Kinase
ddPCR	Droplet Digital PCR
EDDU	Early Drug Discovery Unit
MNI	Montreal Neurological Institute
LNA	Locked Nucleic Acid
ssODN	Single-Stranded Oligodeoxynucleotides
sgRNA	Guide RNA
PAM	Protospacer Adjacent Motif
Indel	Insertions and Deletions
FBS	Fetal Bovine Serum
DMSO	Dimethyl Sulfoxide
hPSCs	Human Pluripotent Stem Cells
FGF-8	Fibroblast Growth Factor-8
BSA	Bovine Serum Albumin
CC3	Cleaved Caspase 3
PFA	Paraformaldehyde
DMEM	Dulbecco's Modified Eagle Medium
M-MLV RT	Moloney Murine Leukemia Virus Reverse Transcriptase
RT-qPCR	Real-Time Quantitative Polymerase Chain Reaction
ICC	Immunocytochemistry

Chapter 1: Introduction and Thesis Overview

Leukodystrophies are a heterogenous group of inherited disorders that affect the white matter of the central nervous system (CNS).[1,2] Most of these disorders are neurodegenerative in nature. There are various types of leukodystrophies, with varying incidence and mortality rates.[10–12] Overall, most leukodystrophies have progressive deterioration after onset and an increased risk of early death.[13] The majority of therapies for leukodystrophies help ameliorate certain clinical manifestations of the disease, while disease modifying therapies are available for only a few types.[12,14–16]

Leukodystrophies are classified as either hypomyelinating or non-hypomyelinating depending on Magnetic Resonance Imaging (MRI) characteristics.[17] RNA Polymerase III-related leukodystrophy (POLR3-HLD) is also known as 4H leukodystrophy, where the "4 H's" represent the three cardinal features of **h**ypomyelination, **h**ypodontia, and **h**ypogonadotropic **h**ypogonadism.[13,18–20] POLR3-HLD arises from biallelic pathogenic variants in genes encoding subunits of RNA polymerase III (Pol III), including *POLR3A, POLR3B, POLR1C, and POLR3K*.[3–7] Elucidating the underlying pathophysiology of how mutations in the Pol III subunits lead to varying presentation of POLR3-HLD will help better understand the wide disease spectrum, ranging from mild to severe forms of the disease.[17]

A cellular model has yet to be developed to study POLR3-HLD, which would allow for visualization of the disease at a cellular and molecular level, and to better understand the underlying pathophysiology. Equally important, it is critical that once such a model is generated, accurate isogenic controls are developed to allow for better understanding of how the specific mutation leads to the phenotype seen in patients, while limiting genetic variability.[21]

In recent years, a severe form of the disease has been described as the severe striatal form of POLR3-HLD. Interestingly, patients with this severe form of the disease harbour a specific genotype with compound heterozygous biallelic pathogenic variants in *POLR3A*, including one allele containing a variant causing a premature stop codon, and the other allele containing an intronic splicing variant.[7] Previous molecular studies done by our research group have shown that the splicing variant is "leaky", producing the wild-type transcript, in addition to two aberrant splicing transcripts.[7] In a previous neuropathological investigation, a patient with a severe presentation showed neuronal abnormalities with progressive involvement of the striatum with insufficient myelin deposition, rather than the diffuse hypomyelination seen in patients with typical POLR3-HLD.[8-11] Of note, in a homozygous state or in a compound heterozygote state with another splicing variant at position c.1771-6 in *POLR3A*, this leaky splice variant lead to striatal involvement without white matter abnormalities, a form now recognized as the mild striatal form.[22] Interestingly, of the 250+ pathogenic variants known to cause POLR3-HLD, no other variant in *POLR3A, POLR3B, POLR1C* or *POLR3K* has been associated with striatal involvement.[22,23] Therefore, it is thought that these aberrant splicing transcripts may have a dominant negative effect on the cells in the striatum due to the high specificity of the leaky splice variants disease forms affecting the basal ganglia.[7]

This project aims to develop a cellular model of the disease using induced pluripotent stem cells (iPSCs) derived from patients' fibroblasts, create isogenic controls with these cell lines, and generate and analyze Pol III transcription in iPSC-derived neuronal cell types to study disease pathogenesis. This research aims to shed light on underlying pathophysiological mechanisms of this disorder and pave the way toward the development of treatment options for patients suffering from this debilitating neurodegenerative disease.

Chapter 2: Review of Relevant Literature

Introduction to Leukodystrophies

Leukoencephalopathies are a heterogenous group of disorders that primarily affect the white matter of the CNS.[24] These diseases can be inherited or acquired, affect individuals of all ages and can be progressive or static in nature.[25–27] Leukodystrophies (*leuko* = white and *dystrophy* = degenerating) are genetically determined leukoencephalopathies with a collective incidence rate of approximately 1:4733, however different subtypes have varying incidence rates.[28,29] By definition, they affect the glial cells of the CNS, including oligodendrocytes, astrocytes, and other non-neuronal cell types, with or without peripheral nervous system involvement.[30] These rare disorders follow a mostly progressive clinical course, with increasing disabilities and eventual death months to years after onset.[29] Patients typically present in infancy, childhood or adolescence with varying levels of motor decline, with or without cognitive and behavioural abnormalities.[13,29,31]

Clinical manifestations, MRI, and targeted genetic investigations, are utilized to aid in accurately diagnosing a patient.[29,30] Recent progress made using MRI technology and molecular genetics have made strides in uncovering various subtypes of leukodystrophies.[29,30] Furthermore, therapeutic advances have also been made, typically to aid in ameliorating debilitating clinical manifestations of the disease, along with some successful restorative treatments.[12–16,29,30] Collectively, leukodystrophies are an under-recognized group of disorders that require further research on their underlying pathophysiological processes.

Classification of Leukodystrophies

A previous leukodystrophy classification system recognized four categories that were distinguished based on the main mechanism of white matter abnormalities.[32] This includes

hypomyelinating (i.e., lack of myelin deposition during development), demyelinating (i.e., a loss of formerly deposited myelin), dysmyelination (i.e., structurally or biochemically abnormal myelin deposition), and myelinolytic (i.e., myelin vacuolization) diseases.[30,32] While this system recognizes the various pathological mechanisms that can contribute to a subgroup of diseases, there may be more cell types involved that play a larger role in the white matter abnormalities seen.[30]

Recent research advances have been made in the pathophysiology of leukodystrophies, regarding the cell types involved in development, maintenance, function, and repair, in relation to pathological changes and pathogenetic mechanisms of white matter abnormalities.[30] This has led to the development of a novel leukodystrophy classification system that is built upon understanding pathological abnormalities and pathogenetic processes.[30] Five categories were generated to better classify leukodystrophies based on the most recent scientific knowledge.[30] The first group is Myelin Disorders, implying that oligodendrocytes and myelin are predominantly affected.[30] Defects that are primarily in astrocyte-specific genes or if astrocyte dysfunction contributes to pathogenesis is classified as the second set, Astrocytopathies.[30] The third category comprises disorders that have myelin involvement due to atypical axon-glia interaction, Leuko-axonopathies.[30] Microgliopathies are the fourth group, encompassing white matter disorders that develop due to defects in genes pertaining to microglia.[30] The last category, Leuko-vasculopathies, includes leukodystrophies that occur due to a vascular pathology.[30]

While this is a largely comprehensive classification system, not all white matter disorders fit into just one category, or some require further research to have their pathophysiology elucidated.[30] Further exploration in disease pathogenesis may aid in understanding the underlying

biological processes encompassing these rare disorders to better classify them, thus allowing for better diagnosis and subsequent treatment of affected patients.[30]

Hypomyelinating and Non – Hypomyelinating Leukodystrophies

Hypomyelinating leukodystrophies refer to disorders that arise due to abnormal myelin deposition during development, while non-hypomyelinating leukodystrophies signify diseases that result from defects in myelin homeostasis.[24] While white matter abnormalities are common between these types of leukodystrophies, the MRI patterns have proven to be distinguishable.[24] A hallmark feature of hypomyelinating leukodystrophies is a slightly hypo-, iso-, or hyper-intense T1-weighted signal of white matter compared to grey matter, while for non-hypomyelinating leukodystrophies there would be a considerably hypointense T1-weighted signal of the white matter relative to grey matter.[24] Both hypomyelinating and non-hypomyelinating leukodystrophies have T2-weighted hyperintensity of white matter, but it is more prominent in patients with non-hypomyelinating leukodystrophies.[24] MRI pattern recognition has proven to have high diagnostic specificity, and also helped defining new disorders and uncovering their causal genes.[24]

Overview of RNA Polymerase III – Related Leukodystrophy

POLR3-HLD is a hypomyelinating leukodystrophy that is characterized by neurologic and non-neurologic features.[18] Originally, five overlapping clinical entities were outlined, and were then renamed to POLR3-HLD due to the causal variants being in genes encoding Pol III subunits, including *POLR3A*, *POLR3B,* and *POLR1C* (identified by Dr. Bernard's research group), as well as the more recently identified *POLR3K*.[3–7] The first was leukodystrophy with oligodontia (LO).[33,34] The second clinical phenotype is ADDH, which represents ataxia (difficulty with maintaining balance and coordination), delayed dentition, and hypomyelination.[35,36] The third is 4H syndrome, where the 4 H's represent the cardinal clinical features of the disease.[13,18–20,37–39] The

first H, hypomyelination, is the key contributor to neurological dysfunction including cerebellar features, pyramidal features, extrapyramidal features, and cognitive impairment.[13,18–20,37–39] The second H refers to hypodontia, for the dental abnormalities that manifest, although oligodontia, delayed dentition, and natal teeth are likewise seen.[13,18–20,37–39] The last 2 Hs, hypogonadotropic hypogonadism, refers to the most commonly present endocrine abnormality, i.e., delayed/absent/arrested puberty, although other endocrine abnormalities can be present.[13,18–20,37–39] Next, hypomyelination with cerebellar atrophy and hypoplasia of the corpus callosum was described as HCAHC.[40,41] Tremor-ataxia with central hypomyelination (TACH) was described as the last presentation.[6,42–44]

Clinical Features and Genetic Etiology of POLR3-HLD

POLR3-HLD is an autosomal recessive progressive neurological disorder with patients experiencing declining motor and cognitive functions.[13,19] Neurological symptoms of the disease include ataxia, dysarthria (slurred speech), tremors, dysphagia, spasticity, dystonia, cognitive difficulties, and in some instances, seizures.[18–20,45,46] Other symptoms include abnormal dentition, absent, delayed or arrested puberty, short stature, and ocular abnormalities (i.e., myopia).[18,19,47] Patients with POLR3-HLD typically also have a characteristic MRI pattern showing hypomyelination with relative preservation of specific structures, including the dentate nucleus, optic radiations, anterolateral nucleus of the thalamus, globus pallidus, and in some patients the corticospinal tracts at the level of the posterior limb of the internal capsule, with or without cerebellar atrophy and thinning of the corpus callosum.[13,18–20]

Genetic confirmation of the disease involves identification of the disease-causing variants typically through next generation sequencing.[48–50] POLR3-HLD can be caused by nonsense variants, missense variants, splice site variants, large exonic deletions, or small insertions or

deletions in four genes encoding Pol III subunits, i.e., *POLR3A, POLR3B, POLR1C* or *POLR3K*.[3,4,7,9,19,20,22,46] With more than 250 known mutations in these genes, with most patients being compound heterozygotes for two different pathogenic variants, it has been challenging to establish genotype-phenotype correlations.[19] However, it has been possible for some variants or combination of variants, and the mild and severe striatal forms of the disease are good examples of this.[9,22,23] It has been shown that mutations in these genes lead to insufficient amount of a subunit produced, impact complex assembly and/or stability through disturbed interactions between Pol III subunits, and/or alter the structure of the catalytic cleft leading to perturbed DNA binding abilities for transcription.[3,6,51,52] To date, there is no record of a patient with 2 null alleles, thus, it is thought that some Pol III expression is required to be compatible with life.[8]

Wide Phenotypic Spectrum of RNA Polymerase III – Related Leukodystrophy

POLR3-HLD has a wide phenotypic spectrum, ranging from mild to typical and severe forms of the disease.[9,19] Patients with a mild phenotype are typically diagnosed in late adolescence or early adulthood and present with learning difficulties and motor clumsiness.[9,19] It is possible that this group is underrepresented, as the mild clinical presentation may make it difficult for patients to obtain an accurate diagnosis. The typical phenotype has been described above but will be summarized here. Patients have an onset before six years of age with a combination of neurological and non-neurological features, typically experience progressive neurodegeneration and death in adulthood.[9,19] Examining the neuropathology of typical patients reveals significant and diffuse decreased myelin with secondary axonal loss and relative preservation of myelin in perivascular regions.[19,31] On the severe end of the spectrum is the severe striatal form of the disease, where patients experience disease onset between 1-3 months of age, with severe developmental delay, regression, and failure to thrive.[9,19]

Clinical data has shown that patients with biallelic pathogenic variants in *POLR1C* have the most severe neurologic phenotype, followed by patients with variants in *POLR3A* and, lastly, patients with variants in *POLR3B* are seen to have milder clinical features.[19,20] Patients with variants in *POLR1C* tend to have the earliest onset of symptoms with the most severe clinical progression, as individuals employed the use of a wheelchair in adolescence and were microcephalic.[20] Patients with variants in *POLR3A* regress rapidly with a shorter life expectancy, however they also experience a later onset of the disease, as compared to patients with variants in *POLR3B*.[19] Furthermore, patients with the mildest phenotypes typically carry the common c.1568T>A mutation in *POLR3B* and most patients of French Canadian descent carried at least one copy of the c.2015C>G mutation in *POLR3A*.[19]

A Cohort of Patients with the Severe Striatal Form of POLR3-HLD

Our group and others have described a severe form of the disease, now recognized as the severe striatal form. Our group reported a cohort of six patients with this severe form of POLR3-HLD with all patients harboring a specific genotype with biallelic pathogenic variants in *POLR3A*, including one allele containing a variant causing a premature stop codon, and the other allele with the c.1771-7C>G intronic leaky splicing variant.[9] We have shown that this "leaky" splice site variant is producing a small amount of the wild-type transcript, in addition to two aberrant splicing transcripts, one lacking exon 14 and the other lacking both exons 13 and 14 of *POLR3A*.[9] Molecular studies on pathological samples from one patient showed a reduction of POLR3A protein levels in the grey and white matter of patients, as compared to control tissue.[9] We therefore hypothesized that, to the contrary to the main pathophysiological hypothesis of a primary oligodendroglial pathogenesis in the typical patients, the severe striatal form of the disease was

rather explained by cell-specific defects involving neurons in the basal ganglia caused by the aberrant transcripts.[9]

Patients were seen in infancy with noticeable feeding difficulties, severe developmental delay, motor regression, and respiratory insufficiency.[9] Half of the cohort had delayed dentition and none were able to achieve independent ambulation.[9] They also developed secondary microcephaly with a combination of axial hypotonia and upper motor neuron signs.[9] The patients had dystonia and chorea, with severe dysphagia requiring an enteral feeding tube.[9,19] Some children in the cohort had ophthalmologic abnormalities, including hyperopia and cortical visual impairment.[9] Endocrine abnormalities were not examined as they succumbed to an early death in childhood due to progressive decline and respiratory complications.[30]

Patients with this severe phenotype have an atypical MRI pattern involving progressive neuronal abnormalities of the basal ganglia and thalami, supratentorial atrophy, and less prominent white matter abnormalities, including mild insufficient myelin deposition, not meeting the criteria required for the diffuse hypomyelination seen in typical POLR3-HLD patients.[9] They presented with T2-hyperintensity of the hilus of the dentate nucleus and T2-hypointensity of the actual dentate nucleus and peridentate region.[9] Brain MRI characteristics demonstrated T2-hyperintensity of the posterior medulla, posterior-inferior pons, and posterior portion of the middle cerebellar peduncles, which suggested axonal degradation.[9] Patients also displayed an irregular signal of the lentiform nuclei and atrophy of the thalami and basal ganglia.[9] Mild to severe supratentorial atrophy was seen, although there were no cerebellar atrophy or pituitary involvement.[9]

In our past studies, neuropathological investigations on a patient with a severe presentation showed neuronal loss especially prominent in the striatum, involving both the putamina and caudate nuclei.[9] Additionally, atrophy of the putamen was evident with severe neuronal loss,

enlarged Virchow-Robin spaces, rare calcifications, and significant activation of microglia.[9] Cellular vacuolization in the thalamus and basal ganglia and decreased myelin in patchy areas of the brainstem and spinal cord were also seen.[9]

RNA Polymerase III Related Disorders

The POLR3-HLD disease spectrum has enlarged significantly in recent years, with disorders that do not necessarily have white matter involvement. One such example is the recently defined disorder caused by *de novo* pathogenic variants in *POLR3B* leading to ataxia, spasticity, sensorimotor peripheral neuropathy, and normal brain myelination, resulting in a clinical presentation distinct from POLR3-HLD.[53] Another example are the patients with biallelic variants in *POLR3B* presenting with isolated hypoonadotropic hypogonadism or endosteal sclerosis.[54,55]

Variants in *POLR3A*, *POLR3B* and *POLR3GL* have been shown to play a role in some cases of Wiedemann-Rautenstrauch syndrome (WRS), a rare disease with heterogenous clinical features.[56–61] While patients with WRS do present with some features similar to that of patients with POLR3-HLD, such as some dental abnormalities (i.e., natal teeth, hypodontia), many manifestations of the disease are distinct.[62,63] Some clinical features common in most patients with WRS include intrauterine growth restriction, poor postnatal growth, facial dysmorphia, lipodystrophy and short stature.[62,63] Subsets of patients present with ocular abnormalities (i.e., myopia, hyperopia), developmental delay, hypotonia, cerebellar signs, muscle weakness, unintelligible speech.[56–58] Additionally, patients with WRS display characteristic facial features (i.e., mandibular hypoplasia, triangular face, widened fontanelles and pseudohydrocephalus) and no hypomyelination, further defining it as distinct from POLR3-HLD.[58]

Three individuals with endosteal hyperostosis, oligodontia, impaired growth, stunted motor skills and dysmorphic facial features were identified as having variants in *POLR3GL*.[64] These

patients had limited neurological impairment and no ocular abnormalities.[64] Two individuals exhibited with delayed puberty, and one patient presented with a thin corpus callosum without hypomyelination.[64]

Certain disorders resembling POLR3-related disorders arise due to biallelic pathogenic variants in genes encoding proteins that interact with Pol III, such as *BRF1*, a subunit of a transcription factor implicated in recruiting Pol III to its DNA targets. The affected individuals present with neurological (i.e., cerebellar hypoplasia, thin corpus callosum) and non - neurological (i.e., dysmorphic facial features, dental abnormalities, short stature) features.

Various disorders with overlapping phenotypic features also arise due to mutations in particular Pol III transcripts.[8] For example, various forms of skeletal dysplasia (i.e., cartilage-hair hypoplasia, anauxetic dysplasia, kyphomelic dysplasia) arise due to hypomorphic mutations in *RMRP* RNA.[65,66] These disorders are characterized by abnormalities in connective tissues resulting in short stature and patients with anauxetic dysplasia have slight intellectual disability and abnormal dentition, while patients with kyphomelic dysplasia have mild facial dysmorphism.[66]

RNA Polymerases

The central dogma outlines a tightly controlled mechanism of the flow of information from DNA to protein, which is essential for the regulation of cell growth, proliferation, survival and apoptosis. Transcription, the fundamental step in gene expression, refers to the process by which genetic information encoded by DNA is used to synthesize RNA molecules. It is governed my numerous regulatory mechanisms that allow for cells to respond to internal and external cues, such as neighbouring cells or cell differentiation signals. Nuclear RNA Polymerases I to III are universally expressed by eukaryotes and each transcribes a specific set of genes from genomic DNA to RNA.[67] RNA Polymerase I (Pol I) plays an essential role in cell growth and survival by

transcribing ribosomal RNA (rRNA) in the nucleolus of the cell.[67] RNA Polymerase II (Pol II) is responsible for the synthesis of mRNA from protein-coding genes.[67] Pol III transcribes small non-coding RNAs (ncRNAs), including all tRNA. Pol III contains 17 subunits, while Pol I and Pol II contain 14 and 12 subunits, respectively.

RNA Polymerase III

Pol III is an essential eukaryotic polymerase with a 10-subunit core and the remaining seven subunits forming subcomplexes important for transcription initiation and termination.[8] Within the 10-subunit core, POLR3A and POLR3B form the catalytic core of the enzyme, two subunits are shared with Pol I (POLR1C and POLR1D), five subunits are shared with Pol I and Pol II (POLR2E, POLR2F, POLR2H, POLR2L, and POLR2K), and there is POLR3K.[8] Of the remaining subunits, POLR3H and CRCP form a stalk complex that's crucial for Pol III initiation, POLR3C, POLR3F, POLR3G, POLR3D, and POLR3E are important for transcription initiation and termination.[8] There are two isoforms of Pol III, depending on whether the POLR3G or POLR3GL subunits are included.[8]

Pol III is responsible for transcribing small ncRNAs that are ubiquitously expressed.[8] It is especially notable for the transcription of *5S* rRNA and transfer RNAs (tRNAs), known for their involvement in protein synthesis.[8] While *5S* rRNA is a part of the ribosome, tRNAs act as a link between the mRNA and growing amino acid sequence during translation.[8] In fact, there are many non-coding RNAs transcribed by Pol III that are implicated in translation and gene expression.[8,68,69] *7SK* RNA transcript indirectly inhibits Pol II transcription and *7SL* RNA serves as a scaffold to target mRNA molecules for secretion by helping direct them to the endoplasmic reticulum.[8] *U6* RNA, *RNAse P* RNA, and *RMRP* RNA are transcripts involved in RNA processing.[8] *U6* RNA forms the active site of the spliceosome and modifies pre-mRNA by removing introns, *RNAse P*

RNA regulates the transcription of tRNAs, and *RMRP* RNA is associated with pre-rRNA processing.[8] *BC200* RNA is expressed exclusively in neurons where it regulates local protein expression.[8] Previous studies have demonstrated that the *BC200* RNA was downregulated in HEK293 cells harboring POLR3-HLD causative mutations, when compared to control samples.[70] Vault RNAs are involved in RNA localization as it contributes to the nuclear pore complex.[8] Y RNAs and Short Interspersed Element (SINE) retrotransposons are Pol III transcripts that are involved in non-canonical roles.[8] Y RNAs may be implicated in inhibiting RNA quality control and are required for initiating DNA replication.[8] SINEs are DNA repeat elements that are commonly found throughout the human genome, however their purpose has yet to be elucidated.[8]

RNA Polymerase III and its Implication in Genetic Disorders

Although ubiquitous expression of Pol III is required during development and throughout life, as it performs an essential role in all cells, disruption of genes encoding its subunits results in distinctive and tissue – specific phenotypes in patients. Biallelic pathogenic variants in various genes encoding Pol III subunits result in a group of neurodevelopmental disorders with varying and overlapping clinical features, including POLR3-HLD.

RNA Polymerase III and Tissue Specific Regulation

There is large genetic and phenotypic heterogeneity seen in Pol III-related disorders, which may be due to different cell types varying in susceptibility to Pol III dysfunction resulting in a diversity of disease mechanisms.[17] For example, cerebral white matter may be a tissue type that is particularly susceptible to decreased Pol III function, due to hypomyelination seen in patients with typical POLR3-HLD.[8] These tissue specific phenotypes seen in various Pol III disorders may arise due to changes in Pol III transcription, which may be caused by Pol III initiation and regulation factors or by altered levels of the multiple essential ncRNAs transcribed by Pol III.[4,8,17,70] Pol III

is a complex and highly regulated enzyme with a critical role in eukaryotic cells, evident through its implication in a variety of disorders.[8]

Cellular Models of Rare Disease

Induced Pluripotent Stem Cells

Disease models allow researchers to better understand disease pathogenesis, which remains largely unknown in POLR3-related leukodystrophy.[9] While animal models have been regarded as viable models for *in vivo* experiments, cellular models can be used to perform robust *in vitro* experiments to visualize the disease at a cellular and molecular levels.[9]

Stem cells are undifferentiated cells that possess the ability to proliferate and differentiate into a variety of lineages.[13] These cells are crucial in development and regenerative processes as they are involved in embryonic development and tissue growth and repair.[21] The several types of stem cells include embryonic stem cells, which are derived from embryos during development, and induced pluripotent stem cells (iPSCs), which are adult cells (i.e., human peripheral blood mononuclear cells (PBMCs), fibroblasts) that are artificially reprogrammed to stem cells with pluripotent capabilities using the four Yamanaka factors: Oct3/4, Sox2, Klf4 and c-Myc.[71]

iPSCs have been implemented in a variety of research applications, including disease modeling, drug discovery, and cell replacement therapies.[21] For example, iPSCs allow researchers to generate disease models from patient-derived cells to allow for *in vitro* examination of cellular and molecular processes.[21] Additionally, in the field of regenerative medicine, iPSCs are promising to replace damaged or diseased cells, as they can be generated from patient cells reducing the risk of rejection or unwanted immune reactions.[21] However, due to this being a relatively new field, further work must be done to ensure the safety of iPSCs.[21] Typically generated using viral vectors,

this opens the door for unwanted tumor generation or unintended genetic abnormalities during the reprogramming process.[21]

Modeling Rare Diseases with Induced Pluripotent Stem Cells

iPSCs allow for researchers to study diseases in a personalized manner as they allow for patient-specific disease models, which is especially useful for rare diseases with small sample sizes.[21,72] This also allows for consideration of the patient's genetic background.[21,72] Additionally, iPSCs allow for recapitulation of underlying pathophysiology as they can be differentiated into specific cell types, such as CNS cells which are difficult to acquire from patients, and then mimic the disease progression *in vitro*.[21,72] Moreover, due to their proliferative abilities, these cells can be expanded so the experiments are reproducible and scalable.[21,72] iPSCs also can be genetically manipulated to introduce or correct mutations to study their effect on disease development and uncover underlying molecular mechanisms or therapeutic targets in a controlled environment.[21,72] Furthermore, iPSCs allow researchers to test potential treatments in patient-specific cells, which would aid in developing improved personalized treatments.[21,72] Using iPSCs to model rare diseases has revolutionized the understanding and treatment of these diseases, which often lack effective therapies due to insufficient understanding of disease pathogenesis.[21,72]

Isogenic and Commercial Controls

A major contributor to iPSCs being valuable disease models is the ability to have isogenic pairs that share the same genetic background, especially of use when studying diseases with large phenotypic variability, like POLR3-HLD.[21] This allows for evaluation of genotype-phenotype correlation in a biologically relevant model. These isogenic controls are generated by correcting the variant in patient-derived iPSCs.[21] Alternatively, when patients' iPSCs are not available, a control cell line can be used and a patient variant may be introduced in that line. With both

approaches, it is crucial to ensure only the one variant is introduced or corrected, without there being any other genetic variability between the isogenic pair.[21] While these controls are the most ideal to use in rare diseases research for disorders with high phenotypic variability, they are difficult to generate and validate.[73–75] Generation of isogenic controls is a relatively new process and while there are established protocols, they must be troubleshooted extensively.[73–75]

Comparatively, commercial control iPSC lines are typically reprogrammed from cells of a healthy individual and then validated to ensure they are pluripotent. These controls allow for speculation surrounding genotype-phenotype correlations in rare disease research, however, they are well-characterized, undergo rigorous quality control, and are extensively studied.[76] These cell lines are reliable and remain consistent cell lines for research, while also being widely available with standardized accessibility.[76]

Using CRISPR/Cas9 Genome Engineering System to Generate Isogenic Controls

The CRISPR/Cas9 genome engineering system is a method that can be used to introduce single nucleotide polymorphisms into the genome of a eukaryotic cell.[108] This system has proven to be useful in generating accurate isogenic controls that are genetically identical except for specific mutations of interest.[77] In this system, the Cas9 endonuclease nicks the DNA, generating a double stranded break, which can be repaired by one of two methods.[77] The first, non-homologous end joining, occurs when the cut DNA gets directly ligated back together.[77] This process is error prone, inefficient, and often improperly incorporates the desired mutation.[77] The latter, used in this project, is homology-directed repair, in which a repair template assists in incorporating the desired mutation.[77] This is a commonly used technique to precisely edit the genome of iPSCs.[77]

Neurons

Neurons are the specialized nerve cells of the nervous system that are responsible for receiving sensory information, transforming the messages into electrical signals and relaying that as motor commands throughout the body. These specialized cells are unique in various ways that allow them to carry out their highly unique role in the CNS, including their morphology.[78] Typical neurons consist of four distinct regions (the cell body, dendrites, axon and presynaptic terminal), that each play a key role in conducting and propagating neuronal signals, also known as action potentials (Figure 1).[79]

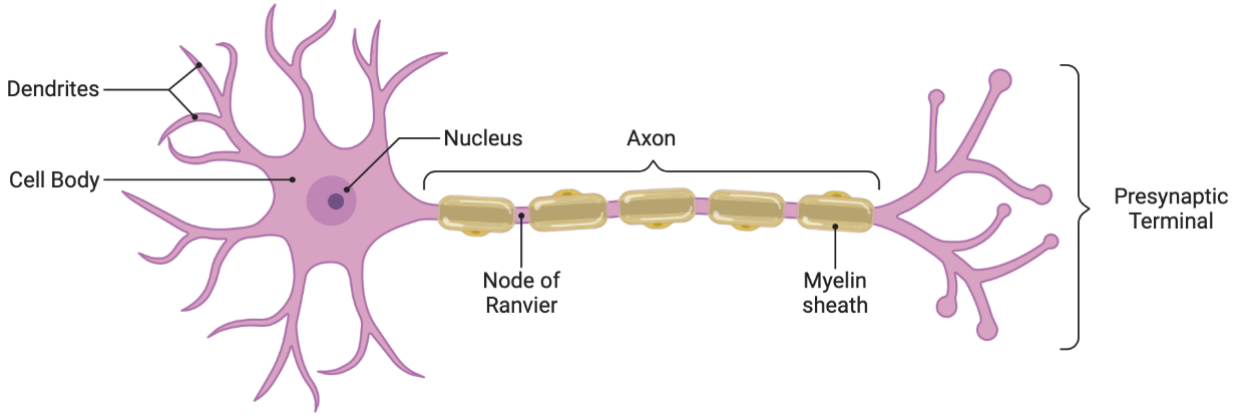

Figure 1. Simplified Diagram of a Neuron. Image made using BioRender.com

The metabolic center of the neuron containing the nucleus is known as the cell body and gives rise to the dendrites and axons.[79] Incoming signals from other neurons are received through the multiple branches of the dendrites while action potentials from the neuron are carried through the axon.[79] Synapses are the zones at which the fine branches of the axon divide to communicate with other neighboring neurons.[79] The synaptic cleft is the space in between the presynaptic terminal (associated with the neuron transmitting the signal) and the postsynaptic terminal (associated with the neuron receiving the signal) where signals are transmitting between neurons.[79] Axons are wrapped in myelin, a lipid substance creating an insulating layer, to maintain the action

potential as it propagates down the axon.[79] These action potentials are regenerated at the nodes of Ranvier, regular intervals where there is an absence of myelin.[79] Various stimuli from the environment can trigger an action potential, and the pathway by which the brain receives and subsequently interprets this information, creates the various sensations experienced.[79]

Development of Neurons

Neuronal development refers to the process by which neurons develop and mature from their early stages in the developing embryo to their fully functional states in the adult organism.[79] The process of neuronal development can be divided into several stages, including neurogenesis, cell migration, differentiation, synaptogenesis, and pruning (Figure 2).[79]

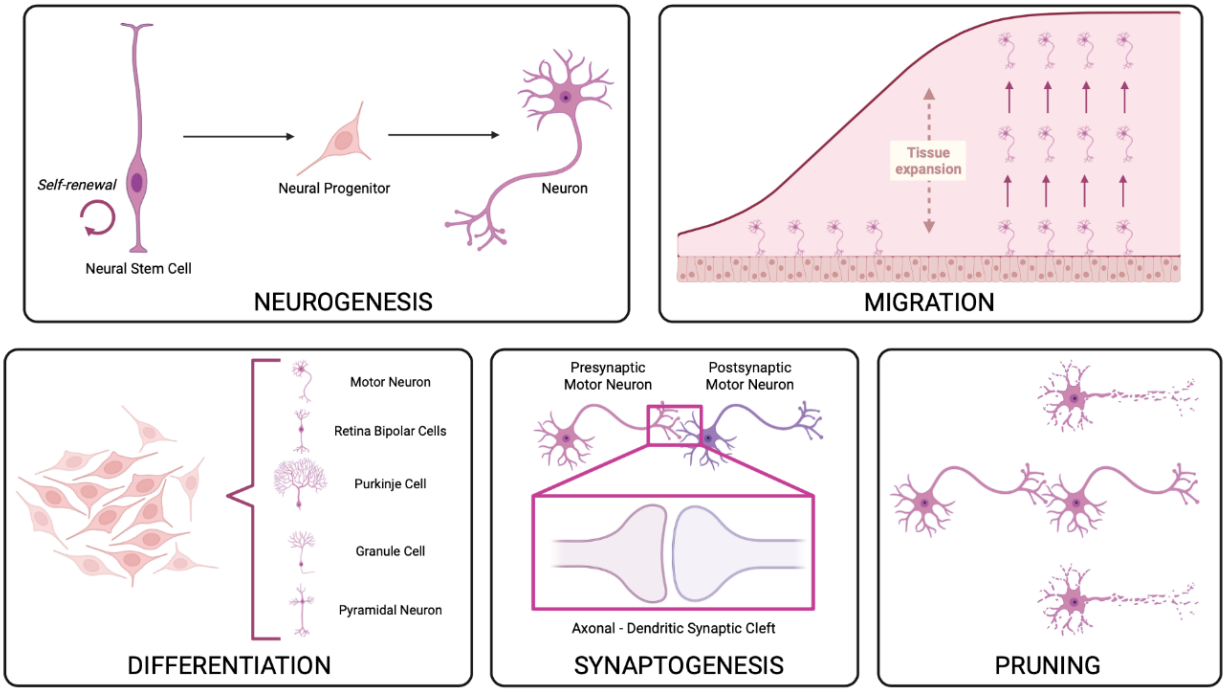

Figure 2. Simplified Schematic Overview of Neurogenesis. Image made using BioRender.com

During neurogenesis, neural stem cells divide and differentiate into neurons.[79] Next, cell migration is the process by which neurons move from their birthplace to their final destination in the brain.[79] Differentiation involves the process by which neurons acquire their specialized

properties, including the formation of dendrites and axons.[79] Synaptogenesis refers to the process by which neurons form connections with other neurons, via synapses, to transmit signals.[79] Finally, pruning refers to the process by which unnecessary or non-functional connections between neurons are eliminated.[79] Overall, the process of neuronal development is a complex and highly regulated process that is essential for the proper functioning of the nervous system.[79]

The Importance of Neural Progenitor Cells in Neurological Disease Research

Neural progenitor cells (NPCs) are a type of specialized stem cell that are multipotent, allowing them to differentiate into different types of glial and neural cells that populate the CNS, including neurons, astrocytes, and oligodendrocytes.[80] *In vitro* studies utilizing the pluripotent potential of iPSCs to develop neurons, involves generating NPCs as an intermediate cell type during neuronal differentiation.[80,81] They are used as a valuable tool for studying the development and function of the nervous system, as well as for developing potential treatments for neurological disorders.[80] Furthermore, deriving this cell type from patients with neurologic disorders, such as POLR3-HLD, allows for visualization of a disease at a molecular level and manipulation of the cell type.[80]

We Hypothesize that Neural Progenitor Cells are Vulnerable to Abnormal RNA Polymerase III Function

The highly proliferative nature and need for differentiation of NPCs requires large amounts of resources, and these metabolic demands must be met to maintain various cellular processes.[80,82,83] For example, processes like DNA replication, transcription, and protein synthesis all require a variety of nutrients, such as amino acids, lipids, and carbohydrates.[80,82,83] Additionally, a large amount of specific growth factors and signaling molecules are necessary to promote differentiation to specific neural cell types.[80,82,83] Due to this, NPC have a high level of Pol III

transcriptional activity to meet their demands, and any disruption may impair neural development and function. [80,82,83]

Utilizing Dual SMAD Inhibition in Vitro to Generate Neural Progenitor Cells

Dual SMAD inhibition is a technique used in iPSC differentiation into specific cell lineages by blocking two specific intracellular signaling pathways.[84] These SMAD pathways are involved in regulating cell differentiation and tissue development, including embryonic development.[84] Dual SMAD inhibition refers to the inhibition of the transforming growth factor beta (TGF-β) and bone morphogenic protein (BMP) signaling pathways using specific small molecular inhibitors, which has proven to efficiently convert iPSCs to neural precursor cells.[84] To mimic this *in vitro*, two small molecules, SB-431542 and dorsomorphin homolog 1 (DMH1), are employed.[85,86] SB-431542 inhibits the activin receptor-like kinase (ALK) 5, which is a TGF-β Type I receptor, and DMH1 is an inhibitor of BMP.[85,86]

Chapter 3: Rationale for the Study, Hypothesis and Specific Aims

Pol III is an essential eukaryotic polymerase and biallelic pathogenic variants in *POLR3A* (among other genes) lead to POLR3-HLD. Isogenic controls are an important aspect of disease modeling as they allow for specific manipulation of the genome to understand how a specific mutation can cause a disease phenotype. Furthermore, the pluripotent nature of iPSCs allow for cellular differentiation to neuronal cell types, that are otherwise extremely difficult to obtain in large quantities for robust experiments. It is unclear as to how the cohort of patients with the c.1771-7C>G intronic splicing variant have a phenotype unlike patients with typical POLR3-HLD and this project seeks to address this gap.

We hypothesize that patient-derived iPSCs are a viable model that can be used to study the pathophysiological mechanisms underlying POLR3-HLD. Additionally, we hypothesize that NPCs derived from patients with severe POLR3-HLD, harboring the intronic splicing variant c.1771-7C>G, will have a specific pattern of aberrant levels of Pol III transcripts.

The project utilizes six patient-derived cell lines and three commercial control cell lines (Table 1 and Table 2).

Table 1. Information about POLR3-HLD Typical and Severe Patient Cell Lines. The patient ID, clinical phenotype, age, sex and *POLR3A* pathogenic variants of the six patient cell lines used in this project are outlined. All iPSC lines were derived from patient fibroblasts.

Cell Line	Clinical Phenotype	Age	Sex (M/F)	*POLR3A* Pathogenic Variants
Patient 1	Typical POLR3-HLD	N/A	M	c.1674C>G; (p.F558L) c.3742insACC; (p.1248insT)
Patient 2	Typical POLR3-HLD	17 years	M	c.2015G>A; (p.G672E) c.2015G>A; (p.G672E)
Patient 3	Typical POLR3-HLD	6 years	M	c.2015G>A; (p.G672E) c.3718G>A; (p.G1240S)
Patient 4	Severe POLR3-HLD	13 months	F	c.1681C>T; (p.R561*) c.1771-7C>G
Patient 5	Severe POLR3-HLD	38 months	M	c.1051C>T; (p.R351*) c.1771-7C>G
Patient 6	Severe POLR3-HLD	21 months	F	c.1051C>T; (p.R351*) c.1771-7C>G

Table 2. Information about the Commercial Control Cell Lines. The names of the control cell lines, age, sex and information about how the commercial control cell lines were generated are outlined.

Control Cell Lines	Age (Years)	Sex (M/F)	Information
Control 1	37	M	Derived from PBMCs using Sendai Virus Reprogramming.
Control 2	50	M	Derived from fibroblasts using Sendai Virus Reprogramming.
Control 3	67	M	Derived from fibroblasts using Sendai Virus Reprogramming.

Our aims for this project were as follows:

1. Generate isogenic controls for the patient-derived iPSC lines using CRISPR-Cas9 genome engineering and droplet digital PCR (ddPCR).
2. Generate and characterize cortical NPCs from severe POLR3-HLD patient-derived iPSCs and control iPSCs.
3. Evaluate Pol III transcription in severe POLR3-HLD patient fibroblasts, iPSCs, and NPCs.

Chapter 4: Materials and Methods

Using CRISPR/Cas9 Genome Engineering to Generate Isogenic Controls

An established protocol developed in the Early Drug Discovery Unit (EDDU) at the Montreal Neurological Institute (MNI) was utilized to develop the CRISPR constructs.[13] The CRISPR/Cas9 Genome Engineering Protocol consists of three main steps: 1. Designing CRISPR/Cas9 Constructs; 2. Clone Picking the Highest Edited Cell Population; and 3. Quality Control of a 100% Edited Cell Line. These three steps were performed in tandem on three separate patient-derived iPSC lines due to them being at different stages of this protocol.

Designing CRISPR/Cas9 Genome Engineering Constructs

For the cells from Patient 1, Patient 2, and Patient 3, the nucleotides of interest (c.1674C>G for Patient 1 and c.2015G>A for Patient 2 and Patient 3) was found on the mRNA sequence from the UCSD Genome database (*POLR3A* NM_007055.3), and then it was subsequently found in the hg19 reference genomic sequence. The DNA sequence was used to design the following constructs: two Locked Nucleic Acid (LNA) probes, ddPCR primers, Sanger sequencing primers, the single-stranded oligodeoxynucleotides (ssODN), and three potential guide RNAs (sgRNA).

The edited nucleotide was detected using a TaqMan® assay with two LNA probes, one which binds the edited allele and the other specific to the unedited allele. OligoAnalyzer™, the IDT thermodynamics calculator, was used to examine the properties of the potential probes designed and to ensure they meet manufacturer guidelines.

NCBI PrimerBlast was used to design ddPCR primers that would surround the LNA probes as well as for designing primers for Sanger sequencing. Additional guidelines followed are outlined in The ThermoFisher Guidelines for Primer Design.[87]

A DNA template with homology arms that flank the codon of interest, ssODN, was designed that contains a nucleotide correction at the variant site, with a silent mutation at the PAM site. The ssODN helps ensure that homology-directed repair occurs when CRISPR editing the iPSCs, as the silent mutation introduced at the PAM helps prevent the repeat cutting by the Cas9 endonuclease.

Designing and Testing Guide RNAs

A guide RNA (sgRNA) is a short RNA sequence that corresponds to the section in the genome where the Cas9 endonuclease should cut. A sgRNA should have a high *in silico* predicted efficiency, minimal off-target effects, and be close to the target variant. The Cas9 nuclease will bind to the region of interest only in the presence of a protospacer adjacent motif (PAM) sequence.[88] The Cas9 endonuclease originating from *Streptococcus pyogenes,* recognizing a 5'-NGG-3' PAM site was used for these experiments, where the sgRNA and Cas9 nuclease were co-delivered into the cell as an RNP complex, rather than as a plasmid, which is reported to have better efficiency.[77,88] Various *in silico* softwares (e.g., Benchling, CHOPCHOP, and CRISPOR) were used to design sgRNAs and to help predict efficiency and potential off-target effects.[89–91]

The sgRNAs designed were tested in an iPSC control cell line to examine editing efficiency by assessing the proportion of insertions and deletions (indel) mutations when no template is provided. Control iPSCs were thawed and passaged into a 6-well plate, until a confluency of 30-40% was reached. Cells were then nucleofected with each sgRNA and once >50% confluency was reached, DNA was collected and Sanger sequencing performed. Chromatograms were analyzed using Synthego's ICE Analysis software. The sgRNA with the highest indel percentage was regarded as the most efficient and was used to correct the mutation found in the patient cells.

Generating Isogenic Controls

An established protocol developed in the EDDU at the MNI was utilized in generating isogenic control iPSC lines from patient-derived iPSC lines.[13] Patient-derived iPSCs were generated from fibroblasts by iPSC Quebec using the Sendai virus reprogramming method, which is reported to have less cytotoxicity and increased reprogramming efficiency.[92] All cell lines underwent pluripotent characterization to ensure good quality and pluripotent capabilities (Table 3 and Figure 3).

Table 3. Techniques and Markers Used for Pluripotency Characterization. The six techniques and respective markers used to confirm the pluripotency of the iPSCs developed by iPSC Quebec are outlined.

Technique	Markers
Immunofluorescence	OCT4, NANOG, SSEA4, TRA-1-60, TRA-1-81
Flow Cytometry	TRA-1-60, TRA-1-81
Differentiation Markers	OCT4 (endogenous), NANOG, SOX2 (endogenous), REXO1, hTERT, DNMT3B
Embryoid Body Formation (16 Day Differentiation) *RNA extraction, cDNA Synthesis, RT-PCR*	Trilineage differentiation: Ectoderm – PAX6, TUBB3, NCAM Mesoderm – SOX17, AFP, GATA4 Endoderm – MSX1, KDR, GATA2
SeV Genome and Transgenes	SeV, KOS, Klf4, c-Myc
Molecular Karyotyping	Chromosome

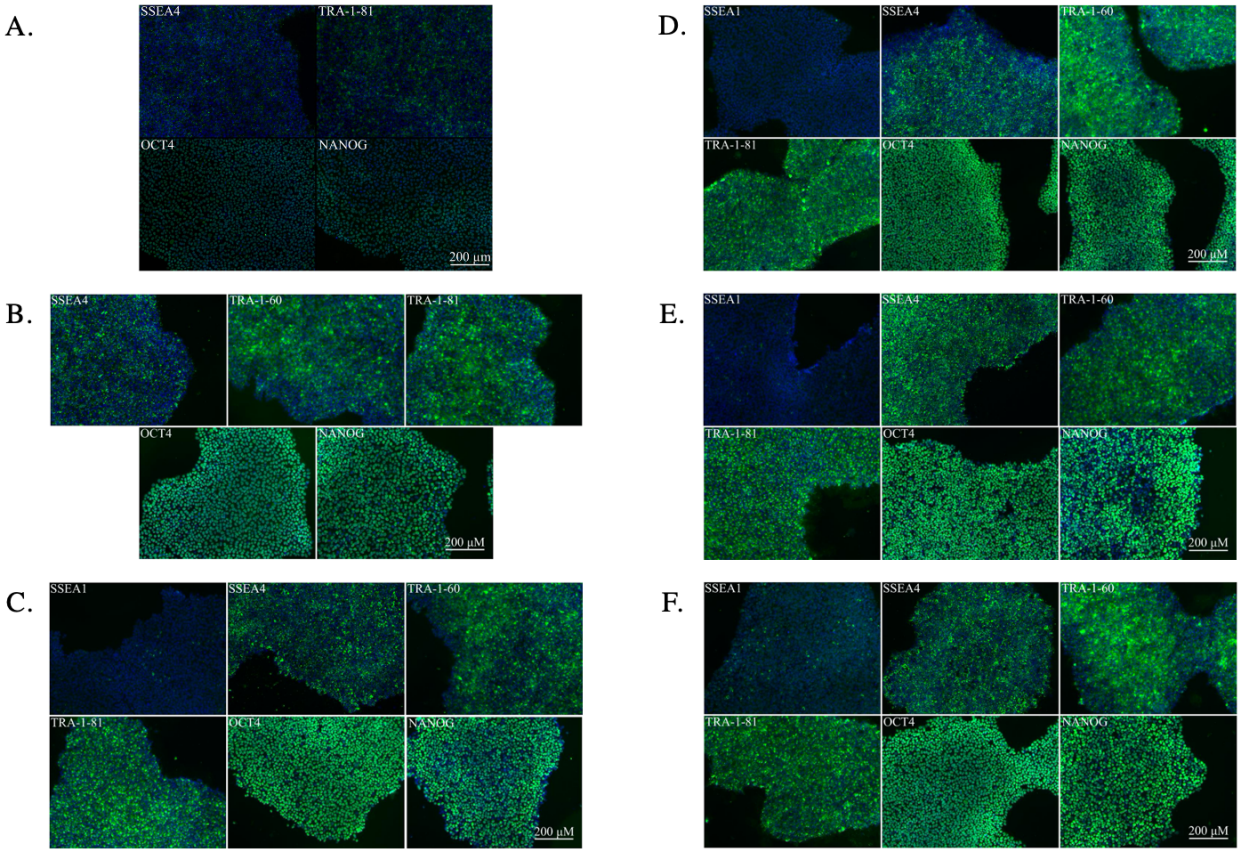

Figure 3. Immunofluorescence Images of Pluripotency Markers for Patient iPSC Lines. Cells were labelled for SSEA1, SSEA4, TRA-1-60, TRA-1-81, OCT4 and Nanog (green). The nucleus is stained with DAPI (blue). Scale bars are 200 μM. **A.** Results for the Patient 1 iPSC line. **B.** Results for the Patient 2 iPSC line. **C.** Results for the Patient 3 iPSC line. **D.** Results for the Patient 4 IPSC line. **E.** Results for the Patient 5 iPSC line. **F.** Results for the Patient 6 IPSC line.

iPSCs were cultured in mTeSR™1 media from StemCell™ Technologies following a previously-described protocol developed by the EDDU at the MNI.[93] Briefly, iPSC cultures were recovered from a frozen stock, cultured in mTeSR™1 media while maintaining appropriate morphology through recurrent passaging, and then were frozen in cryovials in fetal bovine serum (FBS) + 10% dimethyl sulfoxide (DMSO).[93] iPSC morphology was analyzed for a large nucleus with a prominent nucleolus, a large nucleus to cytoplasm ratio, cells that are densely packed, colonies with clear and defined borders, and no differentiated cells or cells growing upwards.[94]

CRISPR components (Cas9 endonuclease, sgRNA, and ssODN) were introduced into cells through nucleofection, an electroporation-based method.[95] The Amaxa™ Human Stem Cell Nucleofector™ Kit 1 was used with the Nucleofector 4D™ Core Unit. Additionally, the Alt-R® HDR Enhancer and Alt-R® S.p. HiFi Cas9 Nuclease V3 from IDT were used. Prior to nucleofection, iPSCs were thawed and passaged to a 6-well plate. 500 000 cells are nucleofected with the RNP complex and subsequently plated into a 96-well plate.

ddPCR technology was utilized to analyze the percentage of edited cells in a cell population.[96] Droplets were first formed in a water-oil emulsion to form the partitions that separate the template DNA molecules.[96] The percentage of edited cells was then analyzed with QuantaSoft by comparing the ratios of FAM and HEX probes, with FAM detecting the wild-type or edited sequence and HEX detecting the patient sequence. The ddPCR process was repeated until a 100% edited line was generated.

Quality Control

Once a 100% edited cell line is generated, it must be expanded, biobanked, and undergo rigorous quality control to validate its quality. Edited cell lines were assessed for pluripotency, genomic integrity, morphology, epigenetic landscape, and marker expression to ensure integrity

of the cells following correction of the pathogenic variant. *In silico* prediction software's Benchling and CRISPOR were used to identify potential off-target sites from the CRISPR-Cas9 editing process. Primers were designed flanking these regions and assessed via Sanger sequencing using SeqMan NGen (Version 12.3.1).[97] To detect genetic abnormalities commonly present in human pluripotent stem cells (hPSCs) that would otherwise be undetectable with G-band karyotyping, a StemCell Technologies hPSC Genetic Analysis Kit was used, following manufacturer's instructions and using a Roche LightCycler Real-Time PCR System and the hPSC Genetic Analysis Application for statistical analysis.[98]

Generation and Characterization of Cortical Neural Progenitor Cells

Generating Cortical Neural Progenitor Cells

Using a previously established protocol developed in the EDDU at the MNI, iPSC lines were cultured and differentiated into cortical NPCs via a 3-week embryoid body suspension culture.[81] Cells were grown in cortical induction media and expanded in NPC Media A with 100 ng/mL fibroblast growth factor-8 (FGF-8) and 1mg/mL 7.5% solution bovine serum albumin (BSA) Fraction V (Figure 4).

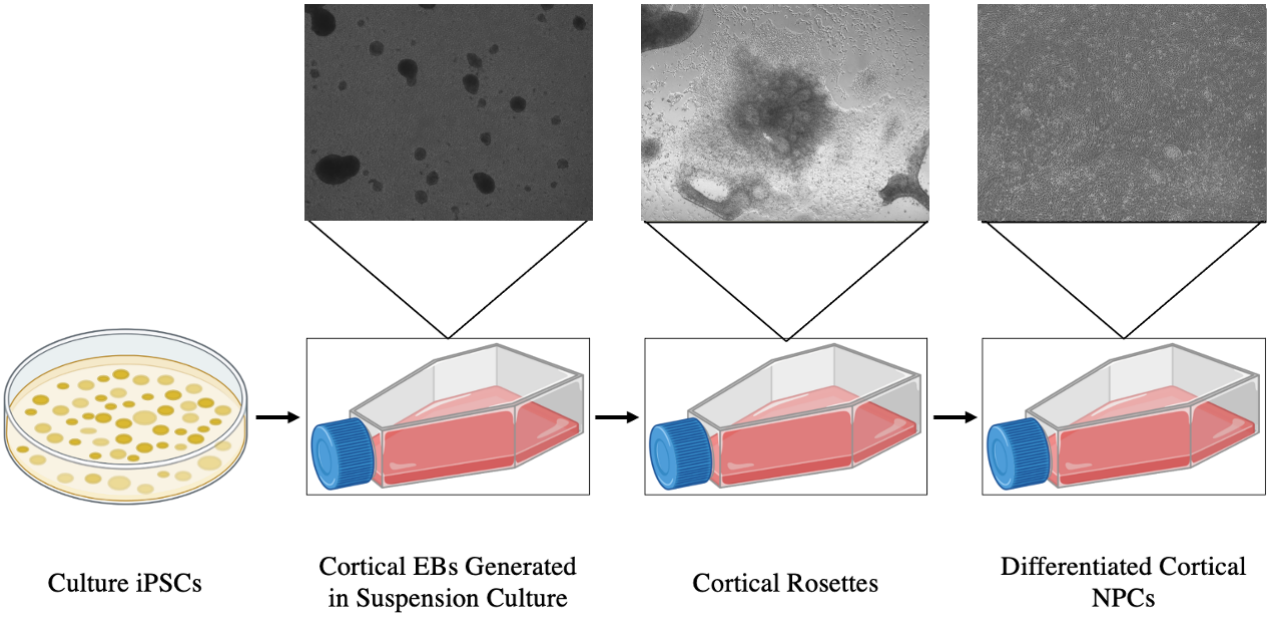

Figure 4. Overview of the NPC Protocol. Cultured iPSCs are generated into NPCs by first generating cortical embryoid bodies in suspension, then cortical rosettes are formed, and finally differentiated cortical NPCs are generated. The three stages in the NPC protocol are depicted in pictures taken throughout the protocol with the commercial control 1 cell line using the EVOS M5000 Brightfield microscope at 4X. Image made using BioRender.com.

Beginning with uncoated flasks to induce embryoid body formation, cells where then transferred onto coated flask to form cortical neural rosettes. Following a passage onto coated flasks for NPC generation, on Day 28, cells were expanded to be biobanked and plated for subsequent RNA extraction and immunocytochemistry analysis. A detailed schematic overview of the protocol is depicted in Figure 5.

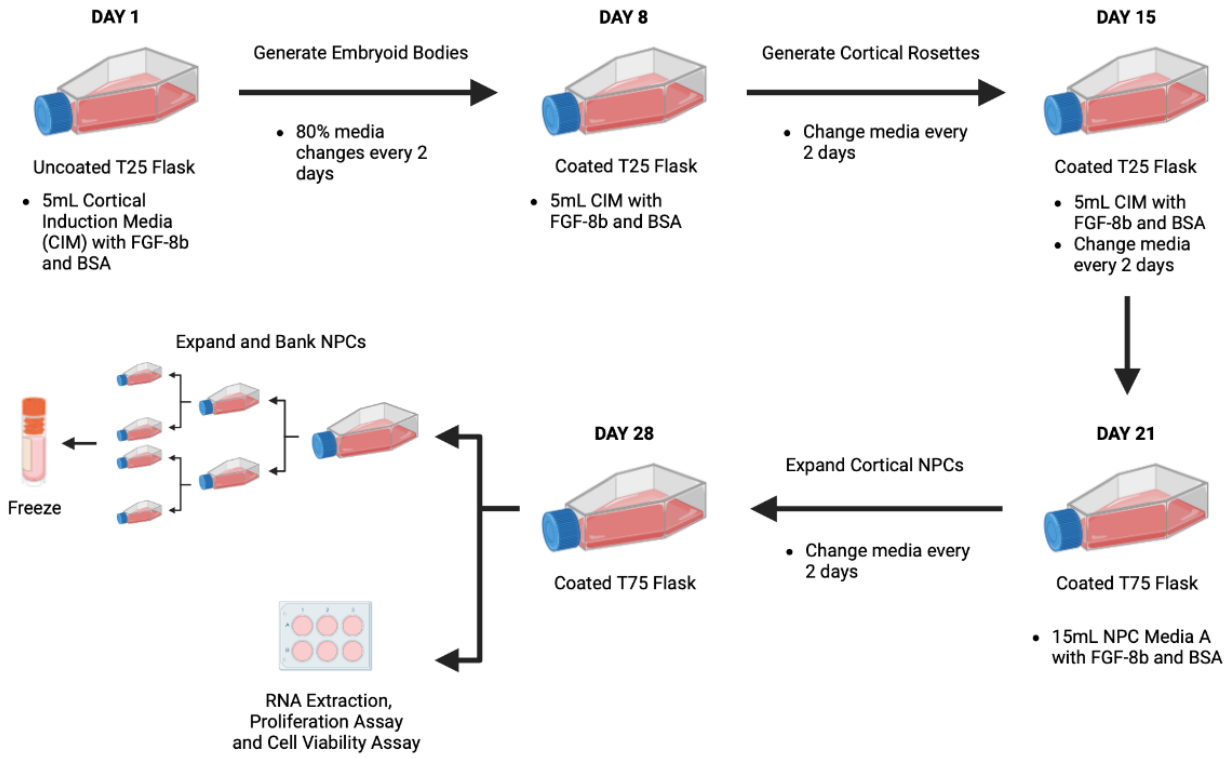

Figure 5. Detailed Schematic Overview of the NPC Protocol. A workflow of how the NPC protocol was executed along with the size of the flask, the number of media changed and the exact days of the protocol each step occurred. Image made using BioRender.com.

Validating Neural Progenitor Cell Generation Using Immunocytochemistry

To ensure the developed NPCs express the appropriate lineage markers, NPCs were stained for PAX6, SOX1, NESTIN, SOX9, and OTX2, markers expressed during overlapping stages of NPC development.[99–105] SOX1 is expressed in neural stem/progenitor cell population, SOX9 is expressed by neural stem cells during embryonic development, PAX6 is a neuroectoderm marker, NESTIN is a marker expressed in a neural stem/progenitor population, and OTX2 is a marker expressed in neural stem cells and it plays a role in the formation of the eyes and related structures.[99–105] Additionally, cell proliferation and viability were assessed by staining for Ki67 and cleaved-caspase 3 (CC3), respectively.[106,107] Cells were counted using the Invitrogen Countless 3 Cell Counter and 100 000 cells were passaged onto coated coverslips. As an overview, cells were

fixed two to three days after Day 28 of the protocol with 4% paraformaldehyde (PFA) for 15 minutes, permeabilized with 0.3% Triton X-100 for 15 minutes and blocked with 0.05% Triton X-100 and 5% BSA for one hour. Cells were then stained with primary antibodies in 0.05% Triton X-100 and 5% BSA buffer overnight (Table 4).

Table 4. Primary Antibody Labeling. The antibody dilution, company, and catalogue number for each primary antibody.

Antibody	Dilution	Company	Catalogue #
Goat anti-SOX1	1:500	R&D Systems	AF3369
Rabbit anti-SOX9	1:500	Millipore	AB5535
Mouse anti-PAX6	1:200	Developmental Studies Hybridoma Bank	PAX6
Mouse anti-NESTIN	1:1000	Abcam	ab92391
Goat anti-OTX2	1:1000	R&D Systems	AF1979
Mouse anti-Ki67	1:250	BD Biosciences	556003
Rabbit anti-CC3	1:400	Cell Signaling Technologies	9661

Following washes, cells were incubated with secondary antibodies in 0.03% Triton X-100 buffer for one hour (Table 5).

Table 5. Secondary Antibody Labeling. The antigen, antibody dilution, company, and catalogue number for each secondary antibody.

Antibody	Antigen	Dilution	Company	Catalogue Number
AlexaFlour488	Donkey anti-mouse	1:500	CedarLane	715-545-150
AlexaFlour680	Donkey anti-goat	1:1000	Thermofisher	A21084
AlexaFlour546	Donkey anti-rabbit	1:500	Thermofisher	A10040
AlexaFlour647	Donkey anti-rabbit	1:500	CedarLane	711-605-152

Cells were imaged using the Nikon Epi-fluorescent microscope and QUPath was used for counting the cells and assessing colocalization. Colocalization was determined by manually counting the cells that co-express all NPC markers with DAPI. This was done in duplicate for each repetition of the NPC protocol. Images were edited using Fiji.

Statistical Analysis

GraphPad Prism (Version 9.4.1) was used for statistical analysis where a one-way t-test was performed with each patient cell line and the control cell lines.

Using Real-Time Quantitative Polymerase Chain Reaction to Evaluate RNA Polymerase III Transcript Levels

Fibroblast Culturing

Patient and control fibroblasts were thawed from cryovials, cultured in Dulbecco's Modified Eagle Medium (DMEM) + 10% FBS and incubated at 37°C. Cells were monitored daily, with media changes done every 2-3 days. Cells were passaged using Trypsin/EDTA once 80-90% confluent. Cells were frozen in a FBS + 10% DMSO freezing solution, with approximately 1 000 000 cells per cryovial.

Sample Collection, RNA Extraction and cDNA Synthesis

RNA was collected from patient and control cell lines at the fibroblast, iPSC, and NPC stage in Qiazol and extracted using the Qiagen miRNeasy Kit with on column DNAse 1 treatment. RNA concentration and quality were assessed using a ND-1000 Nanodrop spectrophotometer. 500ng of RNA was reverse transcribed using Moloney Murine Leukemia Virus Reverse Transcriptase (M-MLV RT), Oligo(d)T, RNAin and random hexamers. 15μL of the primer and RNA template solution is heated to 65°C for 5 minutes to denature the template, which is then cooled to 4°C. After 35μL of the buffer solution is added, the samples were incubated at 25°C for 10 minutes to allow primers to anneal and extent. Next the reaction is held for 60 minutes at 37°C for first-strand synthesis, then inactivated at 70°C for 15 minutes, and finally maintained at 4°C. The synthesized cDNA can be stored at -20°C.

Real-Time Quantitative Polymerase Chain Reaction

Real-Time Quantitative Polymerase Chain Reaction (RT-qPCR) was performed using SsoAdvanced Universal SYBR™ Green supermix. Primers were used to measure the expression of Pol III transcripts including *5S rRNA*, *7SL* RNA, *7SK* RNA, *U6* snRNA, *RNaseP* RNA, *RNase MRP* RNA, htRNA-Leu, htRNA-Tyr, htRNA-Ala, htRNA-Ile, htRNA-Gly, and *BC200* RNA (Table 6) in cells with a 1:40 cDNA dilution.

Table 6. RT-qPCR Primers for RNA Polymerase III Targets. The forward and reverse sequence of the qPCR primers used to detect levels of the seven Pol III targets.

Target	Primer Sequence
5S rRNA	F: GCCATACCACCCTGAACGC R: TATTCCCAGGCGGTCTCCC
7SL RNA	F: GGAGTTCTGGGCTGTAGTGC R: TTTGACCTGCTCCGTTTCCG
7SK RNA	F: CGGTCTTCGGTCAAGGGTATA R: GGATGTGTCTGGAGTCTTGGA
U6 snRNA	F: CGCTTCGGCAGCACATATAC R: TTCACGAATTTGCGTGTCAT
RNaseP RNA	F: GTCACTCCACTCCCATGTCCC R: GGGAACTCACCTCCCCGAAG
RNase MRP RNA	F: AGGCTACACACTGAGGACTCT R: GAAGCGGGGAATGTCTACGT
htRNA-Leu	F: CTCAAGCTTGGCTTCCTCGT R: GAACCCACGCCTCCATTG
htRNA-Tyr	F: AGCGGAGGACTGTAGGTTCA R: GATTCGAACCAGCGACCTAA
htRNA-Ala	F: GGGGAATTAGCTCAAGTGGTAGA R: GGGCATCGATCCCACTACCT
htRNA-Gly	F: GTTGGTGGTATAGTGGTGAGCA R: TGCGTTGGGCGGGAATC
htRNA-Ile	F: GGTTAGCGCGCGGTACTTAT R: TTGAACTCACAACCTCGGCA
BC200 RNA	F: TCTCAGGGAGGCTAAGAGGC R: TGTTGCTTTGAGGGAAGTTACGC

Gene expression of each biological replicate was analyzed in technical replicates and normalized using three reference genes (e.g., *GUSB*, *PGK1* and *TFRC*).

RT-qPCR Primer Design and Validation

NCBI Primer Blast and IDT OligoAnalyzer were used to design the qPCR primers. The reference sequence for the gene of interest was input into NCBI Primer Blast, along with an amplicon size

of 70-150 base pairs and a melting temperature of 55°C-60°C. Once all the primer pair options were gathered surrounding a region of interest, the forward and reverse primer sequences were evaluated by the IDT OligoAnalyzer, indicating an appropriate melting temperature, the highest hairpin temperature being at least 20°C below the melting temperature and a self-dimer and heterodimer free energy above -9 kcal/mole. Primers were validated to meet MIQE guidelines (efficiency between 1.9 – 2.1, $r^2 > 0.95$), using a 1:1 mix of DNA from patient and control cells. Furthermore, it was ensured there is only one melt peak and that amplification curves are evenly spaced out as the serial dilution increases. A sample of the DNA from the qPCR plate at the 1:40 dilution is then run on a 2% agarose gel for 20 minutes at 130V to ensure only one amplified band is seen, fully validating the qPCR primer.

Statistical Analysis

GraphPad Prism (Version 9.4.1) was used to generate graphs and for statistical analysis, where a one-way t-test was performed with each patient cell line and the control cell line.

Chapter 5: Results

Generating Isogenic Controls

Designing CRISPR Constructs for the Patient 1-Derived iPSC Line

Patient 1 carries the c.1674C>G and c.3742insACC pathogenic variants in *POLR3A*. Knowing that parents of affected patients carry one disease-causing variant and are perfectly healthy, correcting only one variant in each cell line should be sufficient to restore wild-type function and obtain isogenic controls. To develop an isogenic control for the line of Patient 1, the c.1674C>G variant was selected as the target due to optimization for correction of single nucleotide changes.[108] Three sgRNAs were generated using in silico predictions (Table 7) and tested in Control 1, to determine which of the three guides was the most optimal for CRISPR/Cas9 genome engineering.

Table 7. Properties of the Three Potential sgRNAs for the Patient 1-Derived iPSC Line. The sequence of each sgRNA, with the nucleotide to be mutated in red, along with the strand and percentage of guanine and cytosine nucleotides. The off-target scores calculated by the *in silico* softwares are given along with the predicted efficiency, provided by CHOPCHOP. The distance from the mutation is also listed. The rank of the guide on each software is outlined as well.

	Guide 1	**Guide 2**	**Guide 3**
Sequence	CACTTT**C**TTTGATCGAG CCAAGG	TGCCTATCTCCTC ACTCTCAAGG	A**G**AAAGTGTCCTTG AGAGTGAGG
Strand	Sense	Sense	Antisense
GC Content	45%	50%	45%
Off – Target Score	Benchling: On-Target Score: 51.9 Off-Target Score: 45.9 CHOPCHOP: MM3 = 7 CRISPR – Tefor: 0-0-0-9-80	Benchling: On-Target Score: 54.1 Off-Target Score: 37.0	Benchling: On-Target Score: 54.7 Off-Target Score: 35.9
Predicted Efficiency	CHOPCHOP: 51.86	N/A	N/A
Distance (base pairs)	10 bp from mutation	12 bp from mutation	15 bp from mutation
Rank	CHOPCHOP: 3 Benchling: 3	Benchling: 2	Benchling: 1

Upon analysis with the Synthego ICE Analysis software, it was determined that sgRNA2 was the most efficient, with an indel percentage of 53% (Table 8). Due to the ssODN not being

introduced to promote homology-directed repair, non-homologous end-joining occurs to repair the double stranded breaks introduced into the DNA by the Cas9 endonuclease. This generates many indels in the target area, leading it to be a good readout of sgRNA efficiency.

Table 8. Synthego ICE Analysis Results. The model fit (Pearson correlation coefficient), indel percentage (editing efficiency) and knockout score (proportion of cells with an indel) calculated by the Synthego ICE Analysis for sgRNA2 and sgRNA3 for Patient 1.

	sgRNA2	**sgRNA3**
Model Fit (R^2)	0.93	0.99
Indel Percentage	53%	6%
Knockout Score	53	3

Since sgRNA2 did not contain the mutation site in the sequence, it did not need to be modified for use with the Patient 1 iPSC line. The ddPCR primers, Sanger sequencing primers, ddPCR probes, and ssODN were also designed (Table 9 and Table 10). The ddPCR probes have different match and mismatch melting temperatures to ensure that the probe is annealed to the template DNA as per the optimal melting temperature set for the ddPCR program. In this protocol, the ddPCR program is optimized for an annealing temperature of 62°C, which is more similar to that of the match melting temperature, rather than the mismatch melting temperature. In the ssODN, the original AAG (Lysine) codon, with a usage frequency of approximately 3.2%, is mutated to AAA (Lysine), which has a frequency of approximately 2.4%.

Table 9. Properties of the ddPCR and Sanger Sequencing Primers for the Patient 1-Derived iPSC Line. The sequence of the ddPCR and Sanger sequencing forward (F) and reverse (R) primers are outlined. The amplicon size and length are given in base pairs, along with the melting temperature (Tm) and percentage of guanine and cytosine nucleotides (GC%).

Primer	**Sequence**	**Amplicon Size**	**Length**	**Tm (°C)**	**GC %**
ddPCR F	CCTAATGCTTAGGTGCCTATCTC	92 bp	23 bp	62	47.8
ddPCR R	GCCAACCAGTATTGAAGCAATG		22 bp	62	45.5
Sanger F	TGAAGTTCACTTGAAAGGAGAT	649 bp	22 bp	60	36.4
Sanger R	CCCACAGACACATACACAC		19 bp	60	52.6

Table 10. Properties of the ddPCR Probes and ssODN for the Patient 1 Derived iPSC Line. The sequence of the probes along with the match and mismatch melting temperatures (Tm) are outlined. The sequence of the ssODN is given with the nucleotide to be mutated in red, the PAM site underlined.

Construct	Sequence	Match Tm	Mismatch Tm
Match Probe (Wild-Type)	A+CTT+T+C+TTT+GAT CG	64.44°C	44.90°C
Mismatch Probe (Patient)	A+CTT+T+G+TTT+GAT CG	66.40°C	52.39°C
ssODN	TctttgttttgtgttggttcctaatgcttagGTGCCTATCTCCTCACTCTCA AAGACACTTTCTTTGATCGAGCCAAGGCTTGCCAAATC ATTGCTTCAATACTGGTTGGCAAGGATGAGAAA	N/A	N/A

Unsuccessful Attempt at Generating Isogenic Controls for Patient 2

To generate a 100% edited isogenic control for Patient 2, both alleles must be edited since the patient is homozygous for the c.2015G>A variant. The percentage of edited DNA is determined through two different probes, FAM and HEX, with absolute quantification through ddPCR. This method quantifies the total amount of patient and isogenic control DNA in each given well, which would mean that for this patient, both alleles would need to be edited to show a 100% edited line. Contrarily, the mutation screening cannot be done such that there is 50% efficiency with homozygous patient lines, as that could imply that 50% of the cells have both alleles edited, rather than half the alleles of all the cells being edited.

As the CRISPR constructs for the Patient 2-derived iPSC line were already designed by a previous lab member, nucleofection and subsequent rounds of ddPCR to identify the highest edited well were performed. Throughout the protocol, cell viability was extremely low with a large portion of cells not surviving the nucleofection procedure. Furthermore, cell viability continued to remain low as the cells were plated into the 96-well plate as single-cell colonies, which was determined through nanodropping the DNA samples prior to undergoing the ddPCR reaction. It was consistently seen that most wells contained DNA with extremely low concentrations,

rendering them unusable for the ddPCR reaction. When the editing efficiency was examined, it remained low despite the highest edited well being continuously expanded. It was evident isogenic controls were proving to be difficult to develop and the protocol needed to be troubleshooted for this patient-derived iPSC line. Troubleshooting these difficulties was attempted by using reagents like ClonR and Gentle Cell Dissociation reagent to promote cell viability in this particularly susceptible patient line. It was hypothesized that editing efficiency remained low as this was the only patient line where both alleles needed to be edited to generate a 100% edited line.

Quality Control for the Patient 3 Isogenic Control iPSC Line Revealed Abnormalities

Although Patient 3 has compound heterozygous mutations in *POLR3A*, only one allele was corrected as POLR3-HLD has recessive inheritance and family members of affected patients harbouring one pathogenic variant are unaffected. As a result, the same CRISPR/Cas9 constructs previously designed to edit the Patient 2-derived iPSC line, were used to edit the c.2015G>A variant in the Patient 3-derived iPSC line. As the editing process had been initiated by another lab member, the plan for this line was to expand the highest-edited wells and use ddPCR to assess efficiency of editing. An efficiency of 100% was achieved in the Patient 3-derived iPSC line. The correction of the c.2015G>A pathogenic variant along with the silent mutations introduced through the ssODN was confirmed with Sanger sequencing (Figure 6). Multiple silent mutations were introduced into this patient line because a single silent mutation in the PAM site was not feasible.

In total, 16 off-target effects were considered for evaluation for the CRISPR edited Patient 3-derived iPSC line (Table 11). The edited DNA sequence was examined using SeqMan NGen, there were no observable changes in the DNA sequence evaluated.

Figure 6. Confirmation of Variants in the Patient 3-Derived CRISPR Edited DNA. The edited c.2015G>A variant and the four ssODN mutation are highlighted in red boxes. The Patient 3-derived CRISPR edited DNA was sequenced twice.

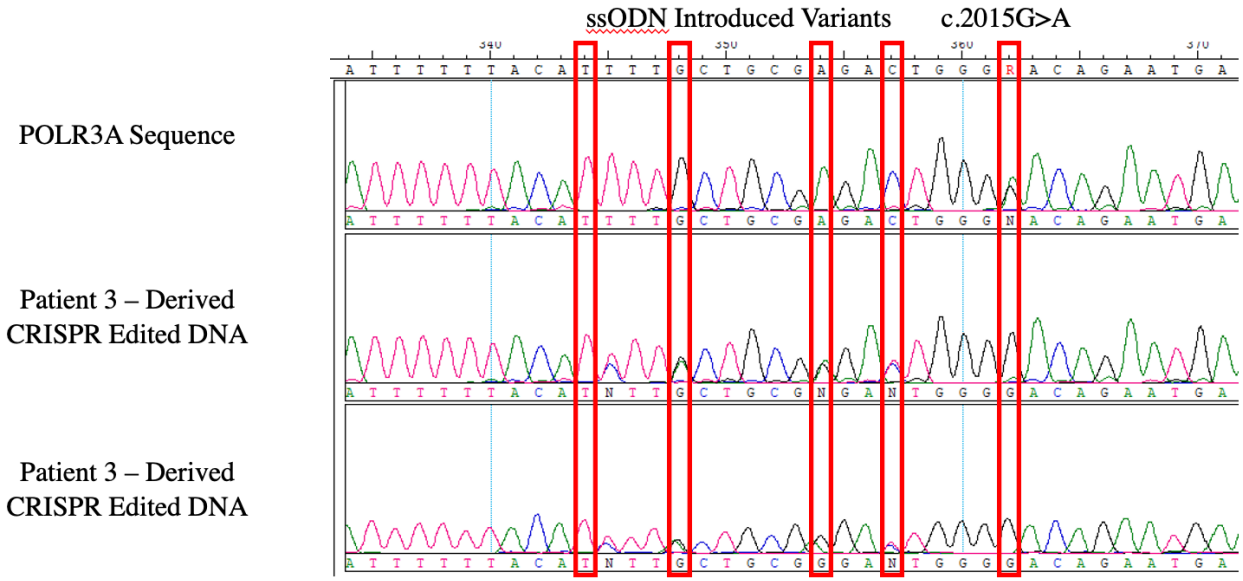

Table 11. Patient 3 Isogenic Control iPSCs Off-Target Effects. The sequences of the 16 off-target effects evaluated for the CRISPR-edited Patient 3 iPSC line are outlined. The PAM, Benchling score, gene, chromosome, strand, position in the genome, mismatches and on-target are also outlined, if available.

#	Sequence	PAM	Score	Gene	Chr	Strand	Position	Mismatches	On-T
0	TTACATTTTGCTGCGAGACT	GGG	100	ENSG00000148606	chr10	-1	79767526	0	FALSE
1	TTGCCTTTAGCTGCGAGACA	AGG	0.51141211		chr8	1	23790378	4	FALSE
2	TCAGATTCTGCTGCAAGACT	AAG	0.47977387		chr11	-1	27999993	4	FALSE
3	TTCAATTTTGCTGGGAGACT	GAG	0.47231235		chr16	-1	83095409	3	FALSE
4	TCTCCTTTTGCTGCAAGACT	TGG	0.46373571	ENSG00000204616	chr6	1	30079495	4	FALSE
5	CTACCTTTTACTGCCAGACT	TGG	0.46037945		chr7	-1	134049804	4	FALSE
6	TGGCATTTTACTGCAAGACT	CAG	0.44923016		chr18	1	65941587	4	FALSE
7	TTTCTTTTTCCTGCAAGACT	TAG	0.42710059		chr12	-1	63164806	4	FALSE
8	TTATATTCTTCTGCCAGACT	CAG	0.40898826		chr3	-1	190987539	4	FALSE
9	ACCCATTTTGCTGCGAGGCT	CAG	0.38037265		chr2	-1	183691519	4	FALSE
10	TTACATTATGCTGCTAGACA	TGG	0.37449101	ENSG00000001629	chr7	1	91924457	3	FALSE
11	TTGGCTTTTGCTGCGAGTCT	TGG	0.35672254	ENSG00000107938	chr10	1	127437108	4	FALSE
12	TGAGATTTTTCTGCGGGACT	GGG	0.29859405		chr5	1	105720694	4	FALSE
13	TGACCTTTTGATGCCAGACT	TGG	0.27173654		chr17	-1	74330895	4	FALSE
14	GTGCATTCTGCTGGGAGACT	CAG	0.2656757		chr8	-1	58535837	4	FALSE
15	AATCATTTTGCTGGGAGACT	CAG	0.25530787	ENSG00000136250	chr7	-1	36656048	4	FALSE
16	NNCAGTCTCGTATCAATATTTAA	N/A	N/A	N/A	N/A	N/A	N/A	N/A	N/A

An initial test with the Genetic Analysis Kit was done for the Patient 3 CRISPR edited iPSC line and it was observed that the edited DNA had putative deletions in chromosomes 8q and 17q and putative amplifications in chromosome 12p and 20q, compared to control DNA provided in the kit. Subsequent tests were performed using the original Patient 3 DNA and the Patient 3 CRISPR edited DNA, to discern how the CRISPR editing process affected the genetic integrity of the cell line. Examination of the Genetic Analysis tests revealed that the Patient 3 DNA had genetic abnormalities in chromosomes 8q, 10p, 12p, 17q, 18q and 20q, while the Patient 3 CRISPR edited DNA had genetic abnormalities in chromosomes 1q, 8q, 10p, 12p and 18q. Due to the high variability between results from these tests, DNA was subsequently purified using the DNeasy Purification Kit. While high variability was still seen, it is likely that the CRISPR editing process introduced a genetic abnormality in a region in Chromosome 8q. Overall, it was concluded that

the integrity of the CRISPR edited DNA was subpar and abnormal by the analysis software (Table 12).

Table 12. Summary of Patient 3 iPSC Genetic Modifications Following CRISPR/Cas9 Genome Engineering. The four tests done on Patient 3 and Patient 3 CRISPR edited DNA are displayed along with a colour coded indication of the status for each chromosome section evaluated. White indicates a normal status, dark red a deletion, light red a putative deletion and light green a putative amplification. The final results from the software are also indicated.

	Test 1	Test 2		Test 3		Test 4	
Genes	**Patient 3 - Edited**	**Patient 3**	**Patient 3 - Edited**	**Patient 3**	**Patient 3 - Edited**	**Patient 3**	**Patient 3 - Edited**
Chr 4p	Normal	Normal	Normal	Normal	Normal	Normal	Normal
Chr 1q	Normal	Normal	Putative Amplification	Normal	Normal	Putative Deletion	Putative Deletion
Chr 8q	Putative Deletion	Normal	Putative Deletion	Putative Deletion	Putative Deletion	Normal	Putative Deletion
Chr 10p	Normal	Putative Deletion	Normal	Putative Amplification	Putative Deletion	Normal	Normal
Chr 12p	Putative Amplification	Putative Amplification	Putative Amplification	Normal	Normal	Putative Amplification	Putative Amplification
Chr 17q	Putative Deletion	Putative Deletion	Normal	Normal	Normal	Normal	Normal
Chr 18q	Normal	Putative Deletion	Putative Deletion	Putative Deletion	Deletion	Normal	Normal
Chr 20q	Putative Amplification	Putative Amplification	Normal	Normal	Normal	Putative Amplification	Putative Amplification
Chr Xp	Normal	Normal	Normal	Normal	Deletion	Normal	Normal
Results from Software	Inconclusive due to Variability Between Replicates	Inconclusive due to Variability Between Replicates		Patient 3: Abnormalities in Chr 8q, Chr 10p and Chr 18q Patient 3 – Edited: Abnormalities in Chr 8q, Chr 10p, Chr 18q and Chr Xp		Inconclusive due to Variability Between Replicates	

Challenges Presented When Generating Isogenic Controls and Future Directions of the Project

Considering the technical difficulties of generating isogenic controls for the Patient 2 and Patient 3 iPSC lines, and the overarching goal of this project, we decided to use commercial controls as a comparator for the severe POLR3-HLD patient-derived iPSC lines. While the increased genetic variability between the patient cell lines and control is a caveat of this study,

developing NPCs and evaluating Pol III transcription with these cell lines will still be a valuable way to assess disease pathophysiology of the severe phenotype.

Measuring Pol III Transcript Levels

Initial Examination Displayed Varied Expression of Some RNA Polymerase III Transcripts in Patient iPSCs and Neural Progenitor Cells

Preliminary results were obtained using all three patient cell lines and Control 1 as iPSCs and NPCs, due to no other commercial cell lines being available at the time and difficulty obtaining good quality RNA samples from control fibroblasts. NPCs with the correct morphology were seen (Figure 7) and the identity of the NPC generated were further confirmed as correct through immunofluorescence (Figure 8).

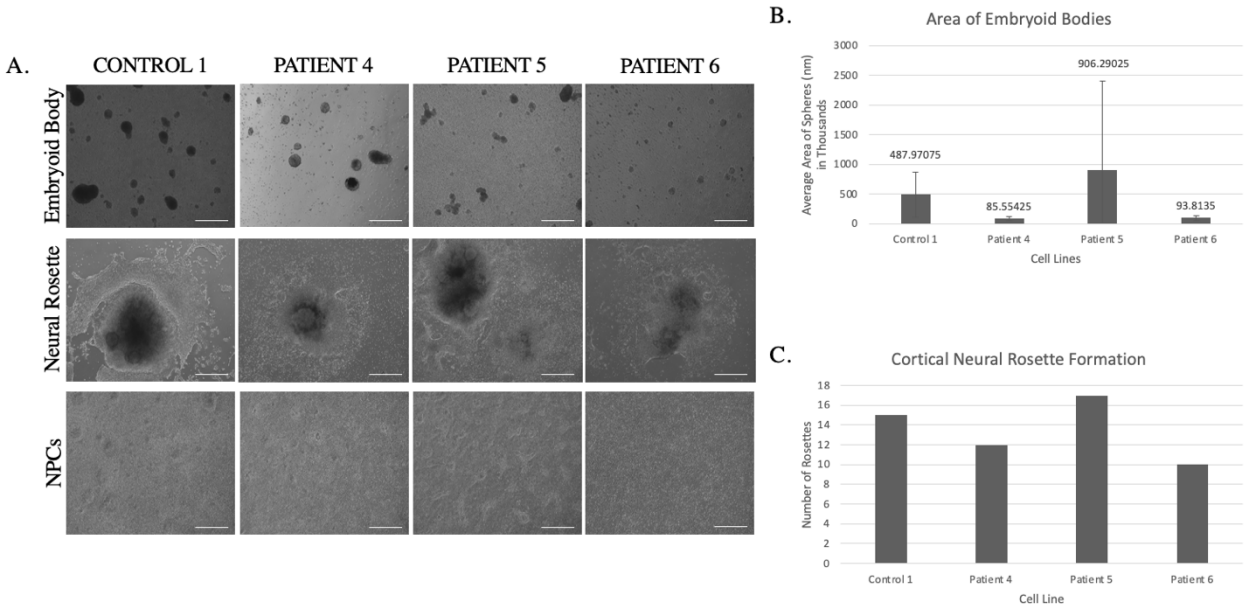

Figure 7. Morphology and Quantification Throughout the NPC Protocol. A. Images of Control 1, Patient 4, Patient 5 and Patient 6 taken at Day 4 (Embryoid Body), Day 12 (Neural Rosette) and Day 28 (NPCs) consistently displaying correct morphology. **B.** Quantification of the average area of the embryoid bodies seen in four random images taken of each cell line on Day 4. Data presented as mean +/- standard deviation, depicts no significant differences between cell lines. **C.** Number of neural rosettes seen in each flask on Day 12.

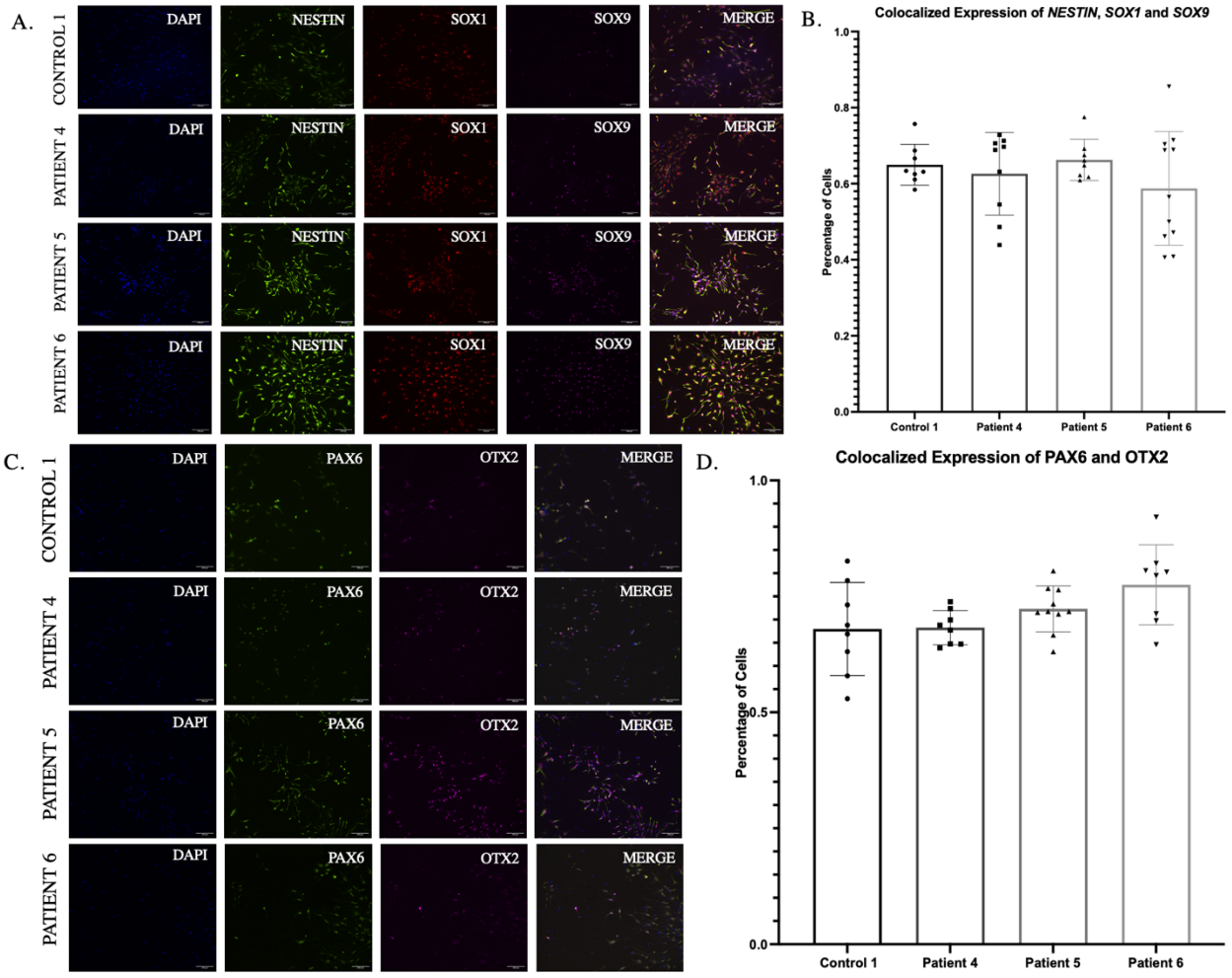

Figure 8. Immunofluorescence Images of NPCs with Common NPC Markers. A. Cells were immunolabelled for NESTIN, SOX1 and SOX9. The nucleus is stained with DAPI. Scale bars are 100 μm. **B.** Quantified colocalized expression of NESTIN, SOX1 and SOX9 showing no significant differences between control and patient cell lines. **C.** Cells were immunolabelled for PAX6 and OTX2. The nucleus is stained with DAPI. Scale bars are 100 μm. **D.** Quantified colocalized expression of PAX6 and OTX2 showing no significant differences between control and patient cell lines.

Examining the proliferative capabilities and apoptosis in the NPCs developed revealed Patient 4 and Patient 5 to be significantly more proliferative ($p<0.0001$ and $p=0.0003$, respectively) and Patient 4 to have significantly reduced apoptosis ($p=0.0012$).

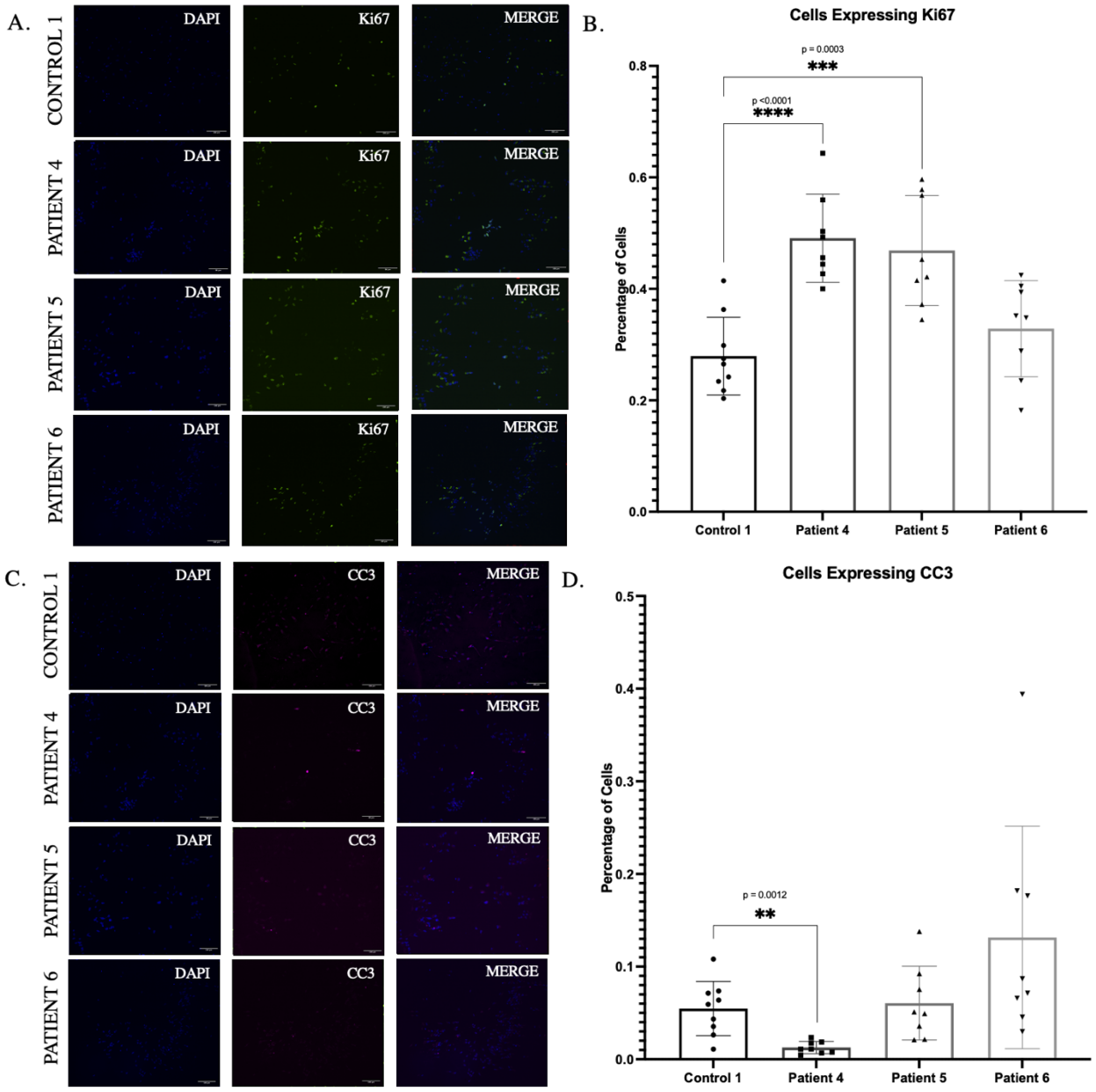

Figure 9. Immunofluorescence Images of NPCs with Proliferation and Apoptosis Markers. **A.** Cells were immunolabelled for Ki67. The nucleus is stained with DAPI. Scale bars are 100 μm. **B.** Quantified colocalized expression of Ki67 and DAPI showing significant increases in Patient 4 and Patient 5. **C.** Cells were immunolabelled for CC3. The nucleus is stained with DAPI. Scale bars are 100 μm. **D.** Quantified colocalized expression of CC3 and DAPI showing significant decreases in Patient 4.

The analysis of Pol III target levels was done using iPSCs and NPCs with Control 1 and cells from Patients 4, 5 and 6 (Figure 10).

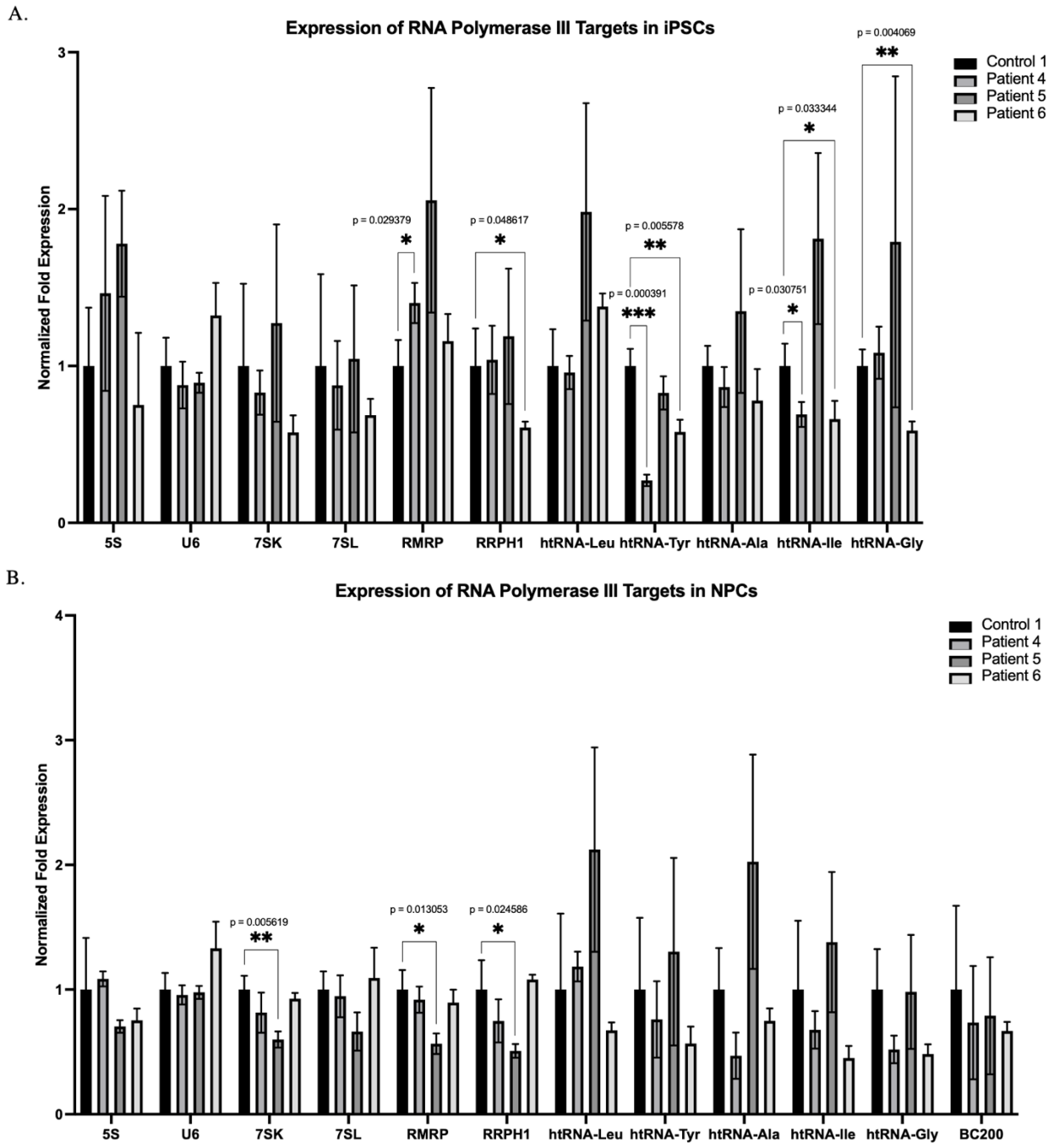

Figure 10. Expression of various RNA Polymerase III Targets in Various Cell Lines. Data presented as mean +/- standard deviation with p-values shown for significant one-way t-tests. **A.** Expression of *5S*, *U6*, *7SK*, *7SL*, *RMRP*, *RRPH1*, *tRNA-Leu*, *tRNA-Tyr*, *tRNA-Ala*, *tRNA-Ile* and *tRNA-Gly* in control and patient iPSCs showing significant differences of varied expression of some Pol III targets. **B.** Expression of *5S*, *U6*, *7SK*, *7SL*, *RMRP*, *RRPH1*, *tRNA-Leu*, *tRNA-Tyr*, *tRNA-Ala*, *tRNA-Ile*, *tRNA-Gly* and *BC200 RNA* in control and patient NPCs showing significant differences of varied expression of some Pol III targets.

In iPSCs it was seen that increased expression of *RMRP* RNA (p=0.029379), which is involved in ribosome biosynthesis, in Patient 4 which may be a compensatory mechanism for decreased tRNA-Tyr (p=0.000391) and tRNA-Ile (p=0.030751) levels. Furthermore, the decreased expression of *RRPH1* RNA (p=0.048617), involved in regulating tRNA expression, in Patient 6 is consistent with the decreased levels of various tRNAs, such as tRNA-Tyr (0.005578), tRNA-Ile (p=0.033344) and tRNA-Gly (0.004069). In NPCs, a decreased expression of *7SK* RNA (0.005619), an inhibitor of Pol II transcription, seen in Patient 5 may be a compensatory mechanism due to decreased expression of *RMRP* RNA (p=0.013053) and *RRPH1* RNA (p=0.024586). No significant differences for tRNAs were seen for any patient cell lines. Large standard deviation error bars seen in iPSCs and NPCs signify variability between biological replicates.

Successful Cortical Neural Progenitor Cell Generation with iPSC Lines from Patients with the Severe Striatal Form of POLR3-HLD and Commercial Controls

To further expand on the previous results seen, the three iPSC lines derived from patients harboring the c.1771-7C>G splice variant combined with a non-sense variant on the other allele, associated with the severe striatal form of POLR3-HLD (Patient 4, Patient 5 and Patient 6) and three commercial control iPSC lines (Control 1, Control 2 and Control 3) were differentiated into NPCs. It was observed that all six cell lines maintained normal cell morphology as iPSCs when cultured and expanded (Figure 11A). At the end of the NPC protocol generation, NPCs with the correct morphology were seen, suggesting that cortical NPCs were successfully generated from the three control and three patient iPSC lines (Figure 11).

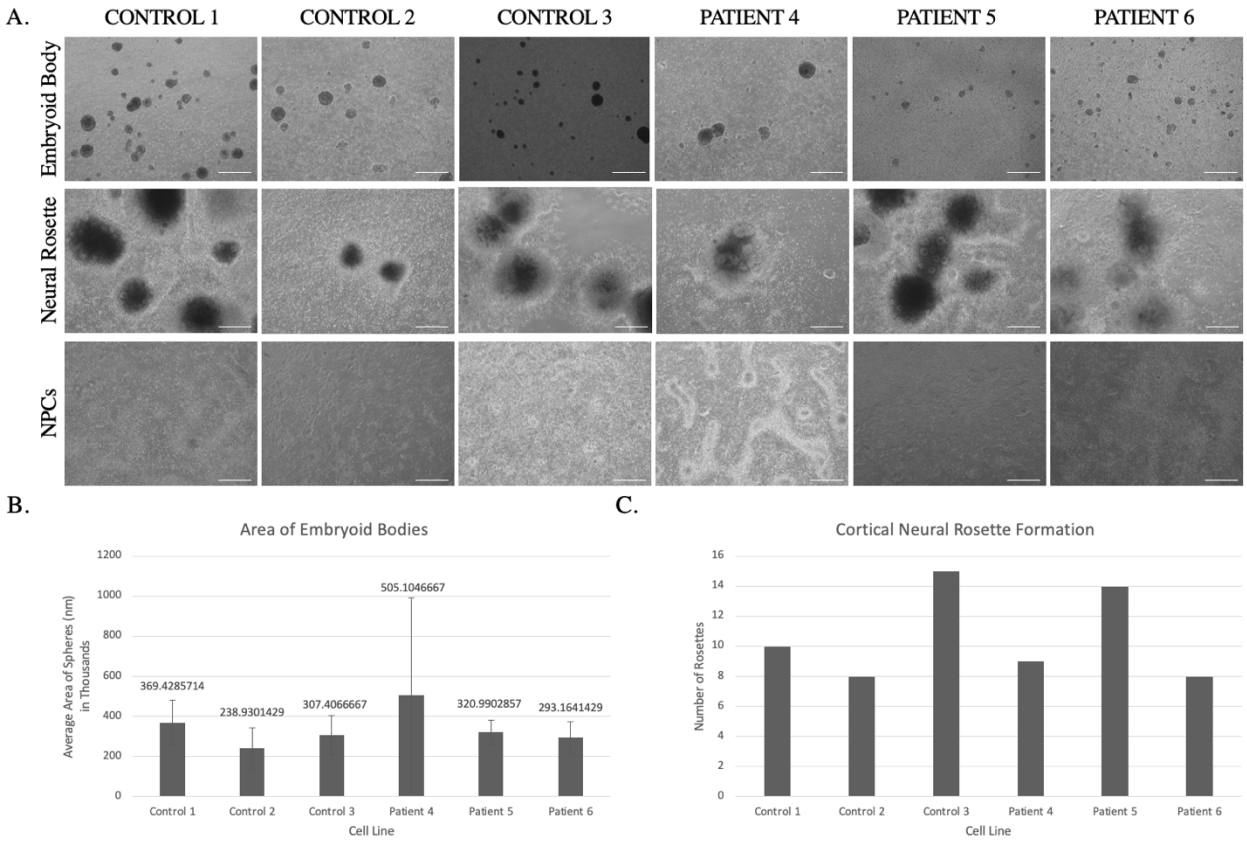

Figure 11. Morphology and Quantification Throughout the NPC Protocol. A. Images of Control 1, Control 2, Control 3, Patient 4, Patient 5 and Patient 6 taken to show embryoid bodies, neural rosettes, and NPCs consistently displaying correct morphology. **B.** Quantification of the average area of the embryoid bodies seen in four random images taken of each cell line on Day 4. Data presented as mean +/- standard deviation, depicts no significant differences between cell lines. **C.** Number of neural rosettes seen in each flask on Day 12.

Validation and Quantification of Neural Progenitor Cells Generated

On Day 28 of the protocol, making the end of the protocol, cells were plated on coverslips and cultured for 2-4 days, at which point they were fixed for immunocytochemistry. Coverslips were imaged and it was observed that the cells from all the lines expressed the appropriate lineage and proliferation markers, further confirming that NPCs were successfully generated (Figure 12). Additionally, comparing the co-expression levels of the NPC markers of each of the patient lines to the control lines indicated that there were no significant differences for any of the markers, proliferative capabilities, or apoptosis indicators (Figure 12 and Figure 13).

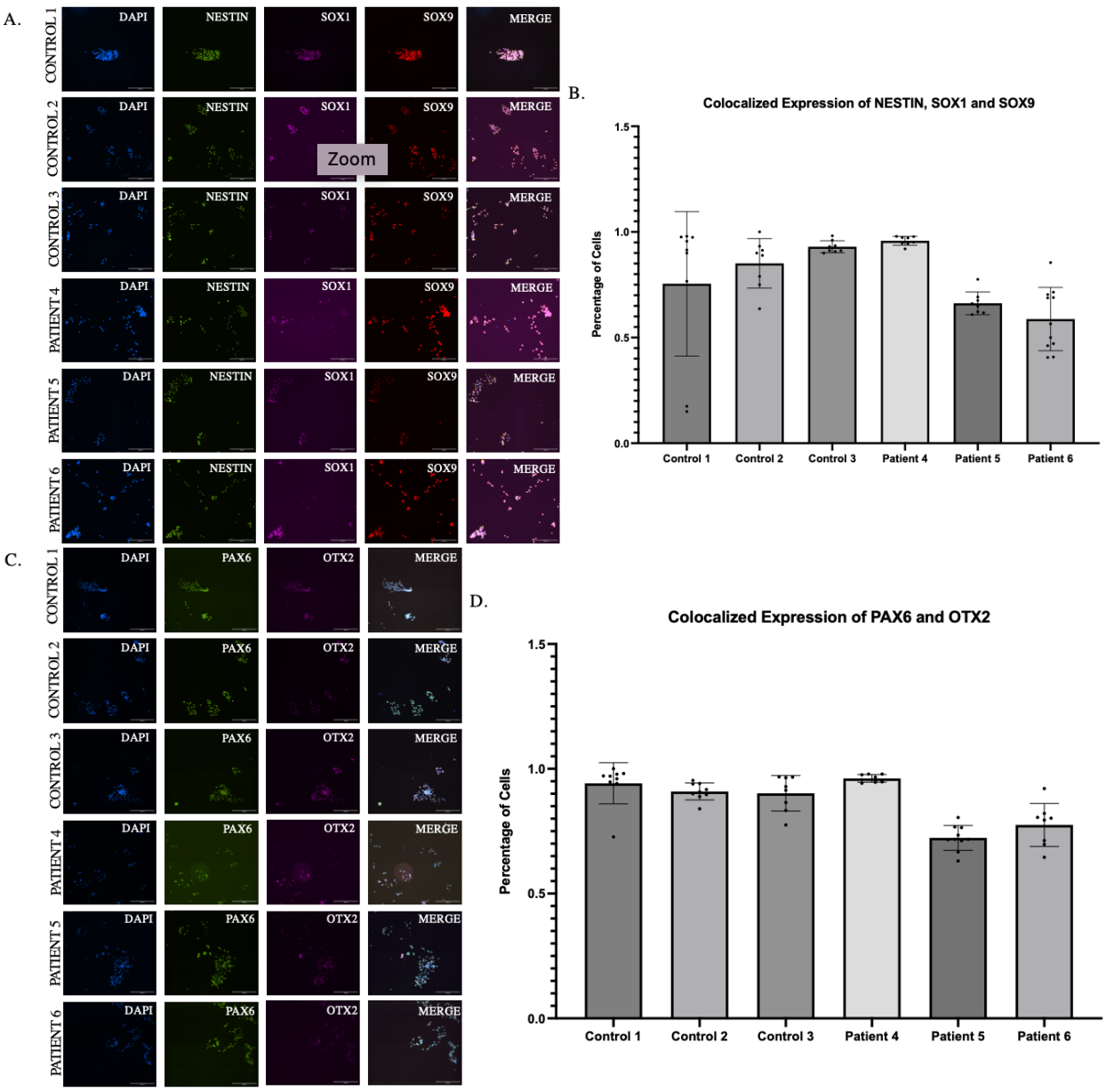

Figure 12. Immunofluorescence Images of NPCs with Common NPC Markers. A. Cells were immunolabelled for NESTIN, SOX1 and SOX9. The nucleus is stained with DAPI. Scale bars are 100 μM. **B.** Quantified colocalized expression of NESTIN, SOX1 and SOX9 showing no significant differences between patient and control cell lines. **C.** Cells were immunolabelled for PAX6 and OTX2. The nucleus is stained with DAPI. Scale bars are 100 μM. **D.** Quantified colocalized expression of PAX6 and OTX2 showing no significant differences between patient and control cell lines.

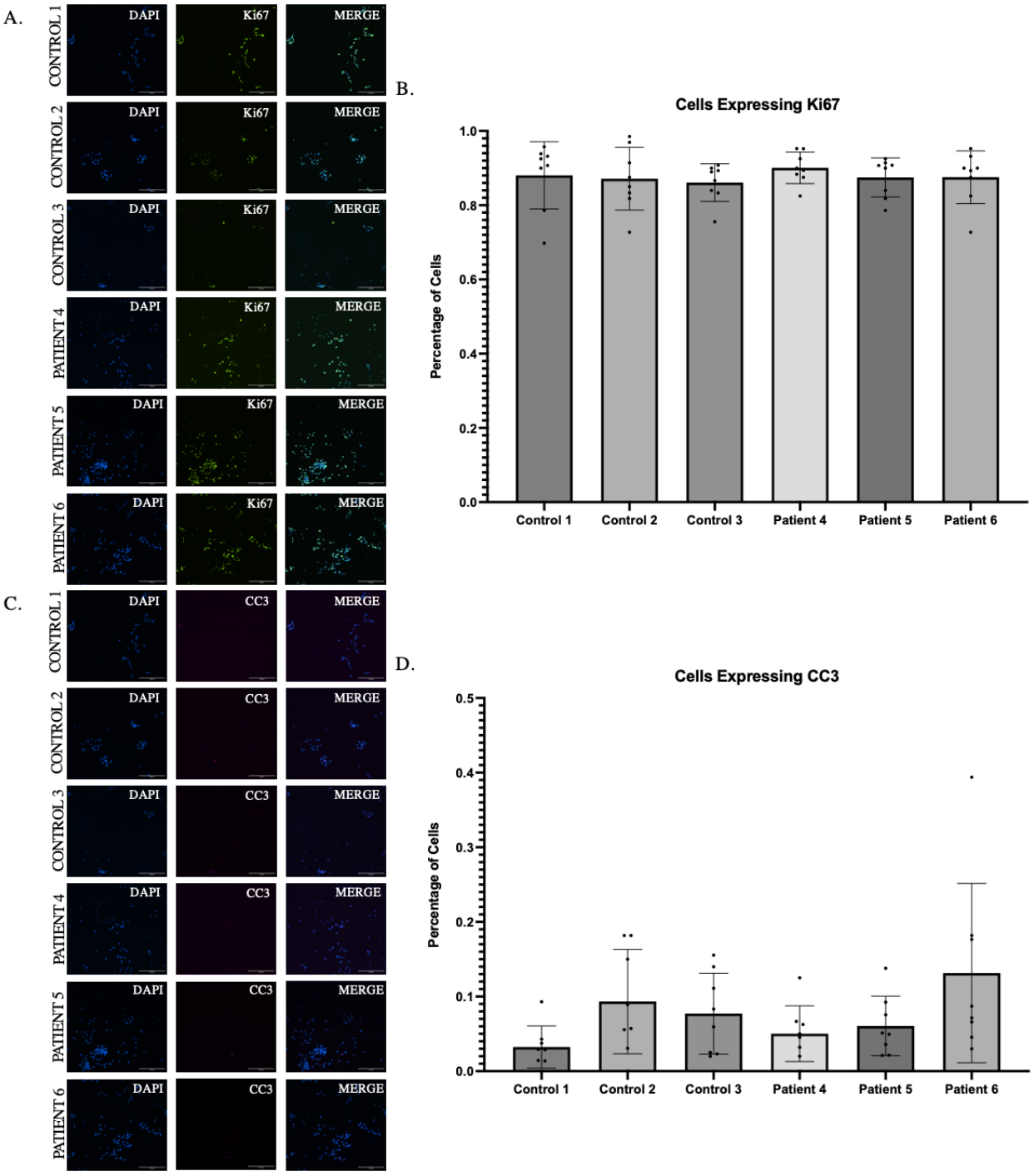

Figure 13. Immunofluorescence Images of NPCs with Proliferation and Apoptosis Markers. **A.** Cells were immunolabelled for Ki67. The nucleus is stained with DAPI. Scale bars are 100 μm. **B.** Quantified colocalized expression of Ki67 and DAPI showing no significant differences between patient and control cell lines. **C.** Cells were immunolabelled for CC3. The nucleus is stained with DAPI. Scale bars are 100 μm. **D.** Quantified colocalized expression of CC3 and DAPI showing no significant differences between patient and control cell lines.

Designing the BC200 RT-qPCR Primer

The reference sequence for BC200 (NR_001568.1) was input into NCBI Primer Blast, and only one primer pair was given and met all the criteria (Figure 14A). The parameters indicated for the thermodynamic properties of the forward and reverse primer sequences were met (Table 13).

Table 13. Thermodynamic Properties of the *BC200* RNA RT-qPCR Primer Pair.

Primer Sequence	NCBI Tm	IDT Tm	Highest Hairpin Tm	Self-Dimer Free Energy	Heterodimer Free Energy
F: TCTCAGGGA GGCTAAGAGGC	60.40°C	65°C	33.5°C	-3.17 kcal/mole	-5.13 kcal/mole
R:TGTTGCTTTGA GGGAAGTTACGC	61.85°C	65.7°C	31.2°C	-3.61 kcal/mole	-5.13 kcal/mole

Various softwares use different algorithms to evaluate primer melting temperatures, which is what accounts for the differences in the melting temperatures from NCBI Primer Blast and IDT OligoAnalyzer.

Upon using RT-qPCR to validate the primer on a sample of mixed control and patient DNA, it was noted that the efficiency was 2.08 and the r^2 value was 0.97, indicating this primer was successfully validated. Along with this, it was noted that there was a singular melting peak (Figure 14B), the amplification curves were evenly spaced apart as the dilution of the cDNA increased (Figure 14C), and the range of Cq values was 23.58 – 28.31.

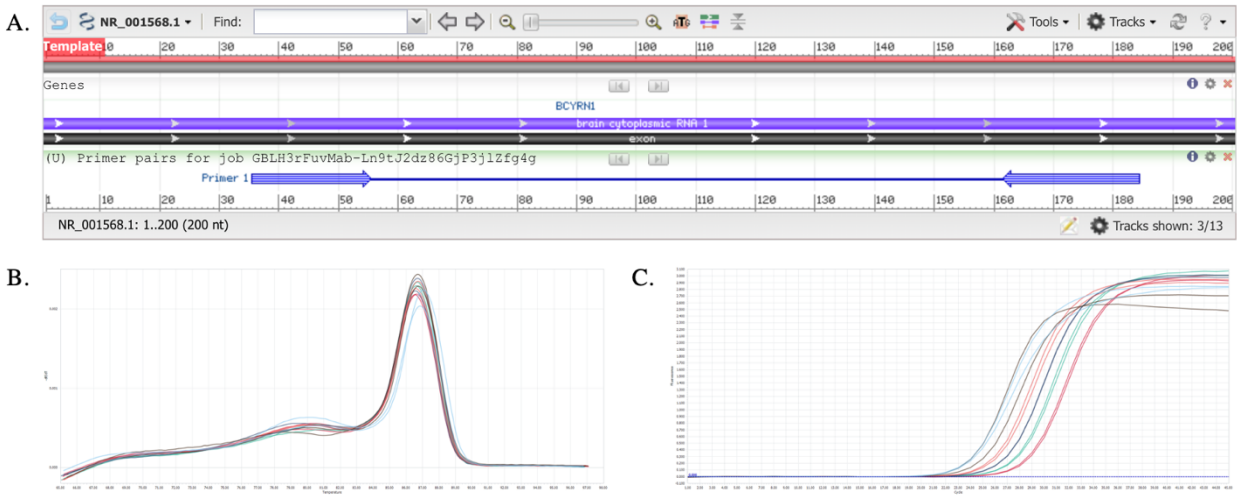

Figure 14. BC200 RNA RT-qPCR Primer Qualities. A. Visual depiction of the placement of the primers on the BC200 RNA sequence. **B.** Graph showing an overview of all the melting peaks for the varying cDNA dilutions. **C.** Graph showing an overview of all the amplification curves for the varying cDNA dilutions.

Additionally, only one band was seen on the agarose gel implying there was only one product amplified, thus fully validating this primer to measure *BC200* RNA transcript levels.

Evaluating RNA Polymerase III Target Levels in Fibroblasts, iPSCs and Neural Progenitor Cells

The analysis of Pol III target levels was done using all three cell types (fibroblasts, iPSCs and NPCs) with Control 1, 2 and 3 and cells from Patients 4, 5 and 6 (Figure 15).

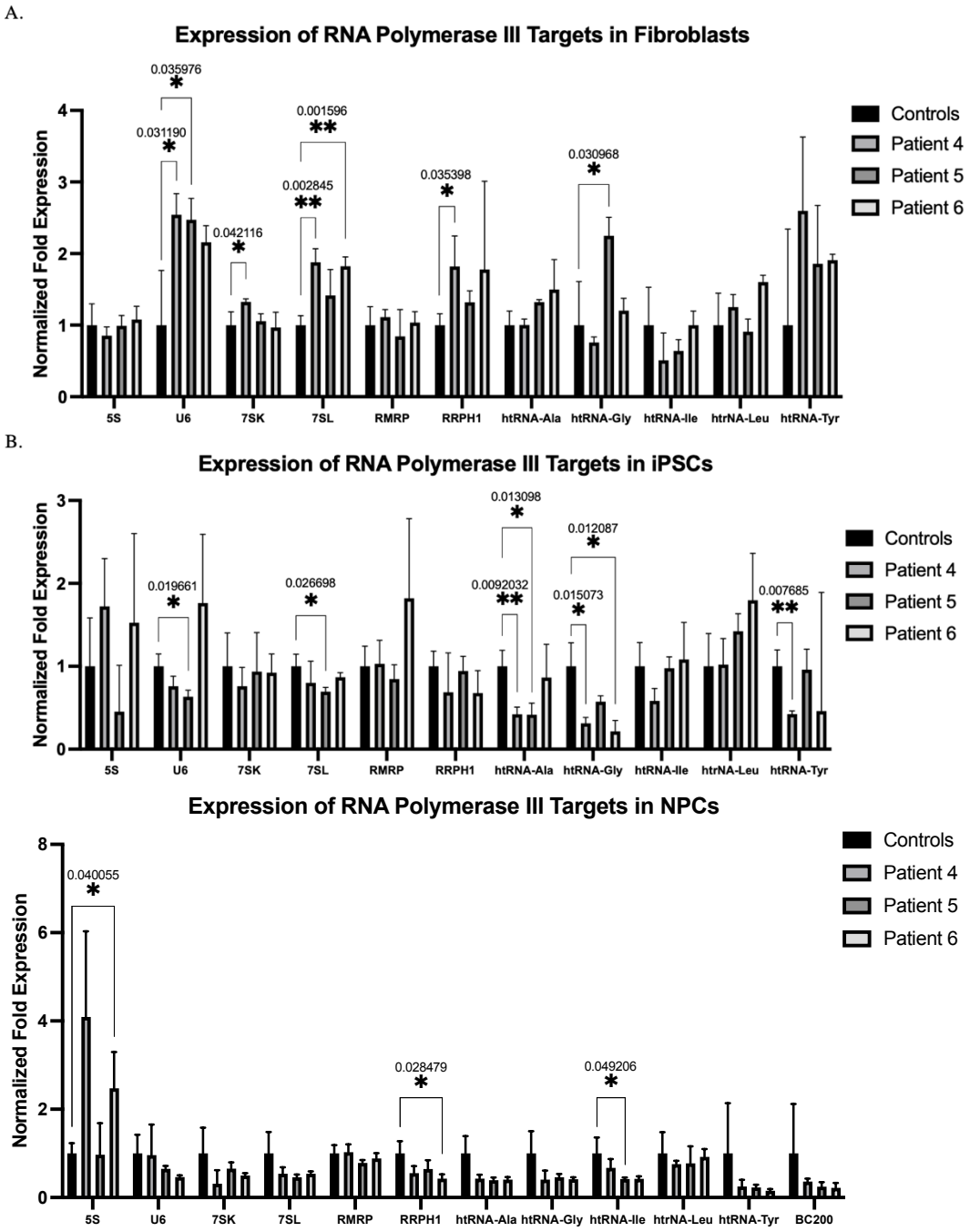

Figure 15. Expression of various RNA Polymerase III Targets in Various Cell Lines. Data presented as mean +/- standard deviation with p-values shown for significant one-way t-tests. **A.** Expression of *5S*, *U6*, *7SK*, *7SL*, *RMRP*, *RRPH1*, *tRNA-Leu*, *tRNA-Tyr*, *tRNA-Ala*, *tRNA-Ile* and *tRNA-Gly* in control and patient fibroblasts showing significant differences of varied expression of some Pol III targets. **B.** Expression of *5S*, *U6*, *7SK*, *7SL*, *RMRP*, *RRPH1*, *tRNA-Leu*, *tRNA-Tyr*, *tRNA-Ala*, *tRNA-Ile* and *tRNA-Gly* in control and patient iPSCs showing significant differences of varied expression of some Pol III targets. **C.** Expression of *5S*, *U6*, *7SK*, *7SL*, *RMRP*, *RRPH1*, *tRNA-Leu*, *tRNA-Tyr*, *tRNA-Ala*, *tRNA-Ile*, *tRNA-Gly* and *BC200 RNA* in control and patient NPCs showing significant differences of varied expression of some Pol III targets.

For the fibroblasts from Patient 4, it was seen that there was increased expression of *U6* RNA (p=0.031190), *7SK* RNA (p=0.042116), *7SL* RNA (0.002845) and *RRPH1* RNA (0.035598), as compared to the controls. *U6* RNA is involved in modifying the pre-mRNA, *7SL* RNA is involved in secreting mRNAs and *RRPH1* RNA is involved in regulating tRNAs, so increased levels of all three indicates increased amount of mRNA transcripts. This also may be a compensatory mechanism due to increased levels of *7SK* RNA, which inhibits Pol II transcription. For Patient 5, there was increased expression of *U6* RNA (p=0.035976) and htRNA-Gly (p=0.030968), as compared to the controls. Lastly, for Patient 6, it was observed that there was increased expression of *7SL* RNA (p=0.001596), as compared to the controls. Patient 5 and Patient 6 both have increased levels of transcripts that help produce and modify mRNAs, which may be a compensatory mechanism for other transcripts that may be implicated further downstream in the Pol III transcriptome.

When expression levels of Pol III transcripts in iPSCs were compared to controls it was seen that there was decreased expression of *U6* RNA (p=0.019661) and *7SL* RNA (p=0.026698) in Patient 5, which may be due to the mutations in Pol III impacting Pol III function, however this may be contradictory to the increased expression of Pol III targets observed in Patient 5 fibroblasts. When looking at the tRNA expression levels, htRNA-Ala is decreased in Patient 4 and Patient 5 (p=0.0092032 and p=0.013098, respectively), htRNA-Gly is decreased in Patient 4 and Patient 6 (p=0.015073 and p=0.012087, respectively) and htRNA-Tyr is decreased in Patient 4 (p=0.007685). Overall, all three patient iPSCs have significantly lower tRNA levels, as compared to control. Additionally, this demonstrates that patient iPSCs have the most significantly decreased tRNA levels, as compared to other cell types.

NPCs from Patient 5 had decreased expression of htRNA-Ile (p=0.049206), while NPCs from Patient 6 had increased expression of *5S* RNA (p=0.040055) and decreased expression of *RRPH1* RNA (0.028479). The increased expression of *5S* RNA, which is a part of the ribosome, may be a compensatory mechanism due to the decreased expression of *RRPH1* RNA.

Overall, it was observed that some Pol III targets were varied in patient cells from all cell types as compared to the controls, with more variability seen in fibroblasts and iPSCs. Furthermore, the large standard deviation error bars seen in all cell lines across all cell types are due to a large variability between biological replicates as there was limited variability seen between technical replicates. While having three control cell lines, instead of one control cell line seen in the preliminary analysis, is important to provide a better baseline for the normalization of the data, this did not help decrease the variability seen for some targets. For example, the expression of htRNA-Tyr in control fibroblasts and NPCs has large standard deviation error bars. This is also the case for htRNA-Gly in fibroblasts, *5S* RNA in iPSCs, and *BC200* RNA in NPCs.

Discussion

The overarching aim of this study was to explore the underlying disease pathophysiology of the wide-spectrum of POLR3-HLD. While the first part of the study involved the use of isogenic controls, which would aid in better understanding how mutations in Pol III lead to POLR3-HLD, the second part of the study involved the study of the expression levels of Pol III transcripts, in hopes to better understand the effects of the c.1771-7C>G intronic splicing variant.

Experimental Difficulties Encountered While Generating Isogenic Controls and Troubleshooting Avenues

Generating isogenic controls proved to be a challenge due to varying editing efficiencies and low cell viability. The low cell survival rate may be due to the nature of the CRISPR/Cas9 genome engineering protocol, which requires the iPSCs to be cultured as single cells, rather than colonies. Additionally, the cells are passaged and ddPCR is performed at the same time for all the wells, regardless of the size of the colonies in that well. This protocol was performed so that most wells contained colonies of the optimal size, while some colonies were smaller, and this could further contribute to the low cell viability as the cells may have been too premature to passage. Moreover, if some of the colonies were too large, there may already be some differentiated cells which would further decrease the amount of viable iPSCs. While the nature of keeping the iPSCs as single cells throughout this protocol cannot be changed, the time point at which the cells are passaged and ddPCR is performed can be optimized for each well. This would ensure that each well is passaged and measured at its optimal time, which would further promote cell survival.

Genetic abnormalities are a common occurrence, typically seen in iPSC lines that have been in culture for extended periods of time and due to CRISPR/Cas9 genome engineering, where extra copies or deletions of specific regions in the chromosome are correlated to an increased

expression of gene(s) that promote cell survival.[109] For example, one of the most common mutations detected in hPSCs is a gain of 20q11.21, which results in an increased copy of several genes, such as *BCL-XL*, which leads to increased cell proliferation.[110,111] There is limited information in previous literature on the significance of deletions seen in the Chr8q, Chr10p and ChrXp regions, as seen in Patient 3.[109] However, deletions in the 18q region may be related to *NOXA*, a pro-apoptotic gene located in the chromosomal region 18q.21.32.[112] *NOXA* encodes a critical domain that is essential for proteins involved in apoptosis and interacts with anti-apoptotic protein to activate Caspase-9, an initiator in the apoptotic pathway.[112] It is hypothesized that the deletion of *NOXA* would decrease the sensitivity of hPSCs to mitotic error and increase the survival of cells with chromosomal abnormalities to increase cell survival during dissociation.[112] While these genetic abnormalities may be a caveat of the nature of the CRISPR/Cas9 genome engineering process, tools like this Genetic Abnormality Detection Kit must be used consistently to evaluate the integrity of the cell lines as they remain in culture.

Harsh reagents like Accutase, are used regularly throughout the protocol to increase cell viability during passaging. While this may overcome one problem, this leads to further problems downstream, as seen by the genetic abnormalities seen with the isogenic control developed for Patient 3. While the results of the Genetic Analysis kit were inconsistent, it was consistently seen that the isogenic control did contain genetic abnormalities not seen in the original patient DNA. While these genetic abnormalities cannot be entirely avoided and are an inherent caveat of the CRISPR/Cas9 genome engineering process, the severity and quantity of the abnormalities is problematic and defeats the purpose of generating isogenic controls. Alternatively, other reagents, such as Gentle Cell Dissociation Reagent, can be employed for use instead of Accutase as a less

harsh method of passaging cells, which would hopefully aid in better cell viability and possibly fewer genetic abnormalities, such as those seen in Patient 3.

Overall, a more comprehensive quality control pipeline needs to be developed that provides consistent and accurate results that give insight to the integrity of any isogenic control line developed. One viable approach is to employ some of the same methods utilized by iPSC Quebec to validate the iPSCs developed from patient fibroblasts (Figure 3 and Table 3). This would be valuable as it would also allow for comparison between the patient cell line before and after the CRISPR/Cas9 genome engineering process. Pluripotency of the iPSCs can be confirmed with immunocytochemistry (ICC) with common pluripotency markers (i.e., OCT4, NANOG, SSEA4, TRA-1-60, TRA-1-81) and trilineage differentiation can be assessed through RT-qPCR with the same markers. The expression of these markers can then be quantified and compared with the patient iPSCs originally received from iPSC Quebec, providing an accurate baseline for the isogenic control.

Generating isogenic control proved to be challenging and while various techniques were used to preserve cell viability while maintaining a high editing efficiency, isogenic controls were unable to be successfully obtained. Although a well-established protocol to introduce an SNP was used, working with patient-derived iPSCs proved to be particularly challenging, especially related to cell viability. This may provide an indication to the fact that mutations in Pol III may impair the survival rate of these cells, as compared to CRISPR/Cas9 genome engineering being used to introduce a mutation implicated in patients with POLR3-HLD into commercial control cells. Due to the time constraints surrounding a master's project, the decision was made to focus on iPSC lines from patients with the severe form of the disease and to use commercial controls to compare the levels of Pol III transcripts.

Varied Expression of Some RNA Polymerase III Targets in Patient Fibroblasts, iPSCs and Neural Progenitor Cells

NPCs were able to be successfully generated from all three patient and all three control cell lines, with no significant differences in co-expression of common NPC markers in between the control and patient cell lines. This may indicate that the abnormal neural defects, seen in previous neuropathology investigations done on tissue samples from Patient 4, may be due to abnormalities downstream of neuronal precursor cell differentiation. While preliminary results did demonstrate increased proliferation in Patient 4 and Patient 5, as compared to Control 1, with Patient 4 also displaying decreased apoptosis, this was not seen when the experiment was repeated with all three control cell lines. This indicates that the significant differences seen in expression levels of the proliferation and apoptosis markers may have been due to a smaller sample size due to only one control cell line being used for comparison to each patient cell line, as these experiments had two biological and four technical replicates.

Preliminary analysis done on the three patient cell lines and just Control 1 demonstrate varied Pol III expression at the iPSC and NPC level, and it was observed that patients have a greater number of targets that were statistically significantly different from controls in the iPSCs compared to the NPCs, which contradicts the hypothesis earlier presented. However, this may be explained by a more downstream effect of the pathogenic variants, which would require performing these experiments in more differentiated cells.

Further analysis done when the experiment was repeated with more control cell lines and fibroblasts demonstrated results consistent with the preliminary analysis. Patient fibroblasts and iPSCs had more Pol III transcripts that were significantly altered as compared to control cell lines, than patient NPCs. It was observed that Patient 4 fibroblasts and iPSCs had the most Pol III targets

that significantly varied from control cell lines, as compared to Patient 5 and 6. Although both Patient 4 and Patient 5 iPSCs had three Pol III targets that were significantly altered from control cell lines, the p-values for the Pol III targets for Patient 4 are lower. For a one-way t-test, the smaller the p-value the less likely that the results occurred due to chance and thus, the greater the significance of the results. Furthermore, patient iPSCs had the most significantly lower levels of various tRNAs, as compared to patient fibroblasts and NPCs, which is consistent with the preliminary results seen. Although Patient 4 is shown to have more Pol III transcript levels significantly altered in fibroblasts and iPSCs, the opposite is seen with NPCs. NPCs differentiated from Patient 4 had no significant differences in any Pol III transcripts, while Patient 6 had the most transcripts altered, which is not the case when evaluating fibroblasts or iPSCs. This result was unexpected as Patient 5 and Patient 6 have the same genotype, and we would therefore had anticipated more similar results when evaluating Pol III target levels. This may be due to several factors, such as epigenetic factors, the patients being of different sexes and/or different age at the time the skin biopsy was performed (38 months for Patient 5 and 21 months for Patient 6). Additionally, there may be differences in the quality of the NPCs derived from iPSCs, with one cell line having a more mixed cell population. Overall, there is no apparent trend seen with one patient line in any of the cell types regarding varied Pol III targets expression.

Large Variability in Biological Replicates May be Due to Mixed Cell Population and RNA Quality

Of note, there was significant variability between biological replicates in the control and patient lines making it difficult to come to any concrete conclusions, which is consistent in both analyses done in all cell lines across all cell types. In NPCs, this may be due to a mixed progenitor population present when the RNA was collected. While the NPC protocol was performed so that

there would be a more mature progenitor population generated, there may still have been immature cell populations present. This is likely the case as when quantified the marker expression for ICC, no cell line displayed 100% colocalized expression, implying that some cells that do not express the markers were present. Furthermore, the quality of the RNA extracted, which was measured through spectrophotometry, for each sample, varied. While most samples have the 260/280 and 260/230 ratios above 2.00, this was not the case for all samples and may be the reason for the variability in results seen for iPSCs and fibroblasts (Table 14).

Table 14. Absorbance Values for RNA Extracted for Samples Used to Evaluate Pol III Transcript Levels. Values in red are highlighted as significant numbers below the 2.00 cut-off value.

Fibroblast Samples	260/280	260/230	iPSC Samples	260/280	260/230	NPC Samples	260/280	260/230
Control 1 - 1	2.04	1.46	Control 1 - 1	2.01	2.00	Control 1 - 1	2.04	2.13
Control 1 - 2	2.03	1.90	Control 1 - 2	1.98	1.98	Control 1 - 2	2.04	1.92
Control 1 - 3	2.03	1.45	Control 1 - 3	2.00	2.02	Control 1 - 3	2.04	2.16
Control 2 - 1	2.06	2.22	Control 2 - 1	2.05	2.01	Control 2 - 1	2.08	1.61
Control 2 - 2	2.05	2.17	Control 2 - 2	2.03	1.37	Control 2 - 2	2.05	1.93
Control 2 - 3	2.06	1.87	Control 2 - 3	2.03	1.59	Control 2 - 3	2.01	1.93
Control 3 - 1	2.05	2.05	Control 3 - 1	2.04	1.94	Control 3 - 1	2.01	1.56
Control 3 - 2	2.05	2.18	Control 3 - 2	2.06	2.23	Control 3 - 2	1.99	1.30
Control 3 - 3	2.05	2.16	Control 3 - 3	2.06	2.21	Control 3 - 3	1.93	0.56
Patient 4 - 1	2.00	1.86	Patient 4 - 1	1.99	1.86	Patient 4 - 1	2.03	1.66
Patient 4 - 2	2.02	1.98	Patient 4 - 2	2.04	2.10	Patient 4 - 2	2.03	2.10
Patient 4 - 3	2.05	2.08	Patient 4 - 3	2.05	2.05	Patient 4 - 3	2.03	2.13
Patient 5 - 1	2.03	2.08	Patient 5 - 1	2.02	2.03	Patient 5 - 1	2.01	1.82
Patient 5 - 2	2.05	1.89	Patient 5 - 2	2.06	1.85	Patient 5 - 2	2.01	1.96
Patient 5 - 3	2.04	2.09	Patient 5 - 3	2.04	2.14	Patient 5 - 3	2.04	1.76
Patient 6 - 1	2.03	2.02	Patient 6 - 1	2.06	2.05	Patient 6 - 1	2.02	2.14
Patient 6 - 2	2.05	2.21	Patient 6 - 2	2.06	2.16	Patient 6 - 2	2.05	2.03
Patient 6 - 3	2.00	1.71	Patient 6 - 3	2.04	1.84	Patient 6 - 3	1.99	2.08

For example, two fibroblast Control 1 samples are below 1.5 and two iPSC Control 2 samples are below 1.6, all of which are considerably below the 2.00 threshold. For NPCs, two Control 3 samples are below 1.5, with one being below 1.0. It would be beneficial to re-extract RNA from these samples to obtain a sample with comparable quality to the rest. One method of overcoming this problem is to continue increasing the sample size, by adding biological and technical replicates. It would be valuable to repeat the qPCR panels, which may help decrease the variation seen.

Implication of Results with Previous Findings

There are several studies that have examined the levels of various Pol III targets, and all have reported decreased levels of varying Pol III targets, whose identity differs in each study. This may be a result of the different variants seen in gene encoding Pol III subunits, the different methodologies used, the different cells studied, and/or the different phenotypes observed in the patients from which the cells are derived.[5,23,70]

The first study performed transcriptome-wide characterization on whole blood cells from patients with the mild striatal variant of POLR3-HLD, homozygous for the *POLR3A* c.1771-6C>G intronic splicing variant, revealing an imbalance in Pol III transcripts.[23] Of note, the phenotype associated with this combination of variants is the mild striatal form and is therefore different from the severe striatal form of the disease studied here. It was seen that global tRNA levels were decreased in patient cells when compared to controls, which is somewhat consistent with the results seen for the patients' iPSCs evaluated in this study.[23] When tRNA levels were further examined, it was determined that htRNA-Gly was the most significantly decreased, with initiator htRNA-Met, htRNA-Leu and htRNA-His also significantly decreased.[23] This is also consistent with what is seen with Patient 4 and Patient 6 iPSCs, although Patient 5 fibroblasts have increased expression. Initiator htRNA-Met and htRNA-His were not evaluated in this study, and it may be worthwhile to examine global levels of tRNA. There was also a reduction in the levels of *7SL* RNA, consistent with Patient 5 iPSCs, although Patient 4 and Patient 6 fibroblasts had increased levels of expression of *7SL* RNA.[23] Furthermore, the study reported increased levels of *RRPH1* RNA, which is consistent with Patient 4 fibroblasts, although Patient 6 NPCs had increased levels of expression.[23] Moreover, the study reported increased levels of *7SK* RNA and *5S* RNA, consistent with Patient 4 fibroblasts and patient 6 NPCs, respectively.[23] Lastly, there was increased

expression of *RMRP* RNA, which was inconsistent with any of the results seen when all three control cell lines were used.[23] However, in the preliminary analysis done with Control 1, there is increased *RMRP* RNA expression in Patient 4 iPSCs and decreased expression in Patient 5 NPCs.

The second study analyzed fibroblasts from patients with a typical POLR3-HLD phenotype with biallelic pathogenic variants in *POLR3K* to evaluate the effect on Pol III targets.[5] Similar to the first study, this study reported decreased levels of *7SL* RNA, and also decreased levels of *5S* RNA.[5] There was also decreased expression of *7SK* RNA, although Patient 4 fibroblasts in this study had increased expression.[5] Lastly, the levels of htRNA-Ala, htRNA-Gly and htRNA-Met were evaluated, and there were significantly decreased levels of the initiator htRNA-Met.[5] This study reported decreased levels of htRNA-Ala in Patient 4 and Patient 5 iPSCs, decreased levels of htRNA-Gly in Patient 4 and Patient 6 iPSCs, and increased levels of htRNA-Ala in Patient 4 fibroblasts, all of which are inconsistent with the results seen in the second study. This is the second study to report decreased levels of initiator htRNA-Met, further promoting the need to measure levels of this transcript in cells from patients with the severe striatal variant of POLR3-HLD.[5,23]

The third study evaluated the levels of the primate-specific neural *BC200* RNA in HEK293 cells with the typical POLR3-HLD causing variant c.2554A>G in *POLR3A* and a null allele.[70] Although *BC200* RNA was not significantly altered in any patient NPCs in this study, the third study reported it as the most down-regulated transcript in fibroblasts and HEK293 cells.[70] Although *BC200* RNA was originally identified only in the brain, it is also expressed in primary and immortalized cell lines at lower levels.[113] Evaluating *BC200* RNA levels in different patient cell types, as fibroblasts or iPSCs for example, can also be done to further evaluate how expression of this transcript is affected by variants in Pol III. Furthermore, *BC200* RNA is hypothesized to be an inhibitor in regulating translation in neural dendrites and is involved in the regulation of alterative

splicing, mRNA stability and translation in p-bodies.[114–116] Overall, this transcript has multiple roles crucial for neural development and would be worthwhile to evaluate in other neural cell types. Lastly, the study reported a global reduction in tRNA levels similar to the first study, and decreased levels of *7SL* RNA similar to the first and second study.[5,23,70]

The fourth study examined the levels of Pol III transcripts in fibroblasts from a WRS patient with the c.3772_3773delCT variant in *POLR3A*.[117] The study demonstrated a decrease in *5S* RNA and *7SK* RNA, but an increase in htRNA-Leu.[117] This is not consistent with the findings of this study where none of our patient fibroblast lines had statistically significant levels of *5S* RNA or htRNA-Leu, and Patient 4 had increased levels of *7SK* RNA. It is interesting to note that in this study the levels of the (only) tRNA measured are increased, while the other studies report a global decrease.[5,23,70,117] These changes may be specific to the WRS phenotype, which is different from the other phenotypes studied but this will need to be further studied with larger numbers of patients, measure of a greater number of targets in different cell types.

The last study assessed the levels of the *7SL* RNA transcript in fibroblasts from a POLR3-HLD patient revealing no significant differences in *7SL* RNA levels, as compared to a control.[118] This is again inconsistent with the findings of this study as Patient 4 and 6 both have increased levels of this transcript. It is important to note that while the patient was reported to display severe neurologic manifestations of the disease, the phenotype is distinct to that of the severe striatal form of POLR3-HLD.[118] Again, it may be that different phenotypes have a specific pattern of abnormal transcript levels.

Altogether, the findings of our study are consistent with first three studies mentioned in that patient cells of all types did have significant decreases in varying Pol III targets as compared to controls.[5,23,70] It would be interesting to further evaluate the levels of tRNAs, either through

examining global or individual levels, and *BC200* RNA in various cell types, including fibroblasts, iPSCs and other more neuronally differentiated cell types. Furthermore, it is important to note the variability in phenotype and genotype of the patients evaluated in the aforementioned studies. While comparisons can be made when evaluating Pol III transcript levels amongst Pol III disorders, the results may vary according to the different phenotypes and cell types studied, as well as the different methodologies used.

Limitations and Future Directions

A limitation of this study is the inability to extract RNA from all the samples together. Indeed, RNA from the samples was extracted in three separate batches, i.e., one per cell type. Additionally, the commercial control fibroblast cell lines used differed from the commercial control iPSC lines used. This does result in inevitable genetic variability between the controls used to compare the patient fibroblast samples with the control samples used to compare the patient iPSCs and NPCs. Moreover, due to limitations in the commercial control lines available, they were unable to be age and sex matched to the patient-derived cell lines. Furthermore, qPCR was done using primers designed in-house, limiting the number of RNA targets that can be evaluated. Other methods, such as doing RNA-sequencing would allow for better understanding of the impact of mutations in Pol III on the transcriptome.

It may be worthwhile to further differentiate the patient and control cells further, to further assess Pol III transcript levels. The NPCs that were generated and subsequently biobanked can be further differentiated into cortical or dopaminergic neurons. Furthermore, the generation of organoids may be considered. It may be interesting to examine and compare the levels of Pol III targets in typical and severe patient cells differentiated into the neural and glial lineage, due to the

patients with severe POLR3-HLD having more neuronal abnormalities and the patients with typical POLR3-HLD displaying frank hypomyelination.

Overall, this project has shown data on the levels of Pol III transcripts in patient cell lines in three different cell types, with evidence showing that the levels of some Pol III targets are decreased as compared to control in all three cell types. Although drastic conclusions cannot be made from this data alone, this project has shown the need for better cellular models to increase our knowledge of the underlying disease mechanisms seen in POLR3-HLD.

Conclusion

POLR3-HLD has a wide disease spectrum and disease pathophysiology is still largely unknown. Developing a cellular model of the disease with patient-derived iPSCs will be a great asset to study disease pathogenesis. Although the technical difficulties in generating isogenic controls have led us to use commercial controls, what we learned along the way will be helpful for future iPSC projects in which generation of isogenic controls will be necessary. This study looking at fibroblasts, iPSCs, and NPCs is the first addressing disease pathophysiology of the severe form of the disease. It is hoped that this research will initiate further studies that will aid in deepening our understanding of the impact of specific mutations in Pol III subunits on Pol III function and the relation between these mutations and disease phenotypes.

References

1. Choquet K, Yang S, Moir RD, et al. Absence of neurological abnormalities in mice homozygous for the Polr3a G672E hypomyelinating leukodystrophy mutation. *Mol Brain*. 2017;10(1):13. doi:10.1186/s13041-017-0294-y

2. Köhler W, Curiel J, Vanderver A. Adulthood leukodystrophies. *Nat Rev Neurol*. 2018;14(2):94-105. doi:10.1038/nrneurol.2017.175

3. Bernard G, Chouery E, Putorti ML, et al. Mutations of POLR3A Encoding a Catalytic Subunit of RNA Polymerase Pol III Cause a Recessive Hypomyelinating Leukodystrophy. *Am J Hum Genet*. 2011;89(3):415-423. doi:10.1016/j.ajhg.2011.07.014

4. Thiffault I, Wolf NI, Forget D, et al. Recessive mutations in POLR1C cause a leukodystrophy by impairing biogenesis of RNA polymerase III. *Nat Commun*. 2015;6(1):7623. doi:10.1038/ncomms8623

5. Dorboz I, Dumay-Odelot H, Boussaid K, et al. Mutation in *POLR3K* causes hypomyelinating leukodystrophy and abnormal ribosomal RNA regulation. *Neurol Genet*. 2018;4(6):e289. doi:10.1212/NXG.0000000000000289

6. Tétreault M, Choquet K, Orcesi S, et al. Recessive Mutations in POLR3B, Encoding the Second Largest Subunit of Pol III, Cause a Rare Hypomyelinating Leukodystrophy. *Am J Hum Genet*. 2011;89(5):652-655. doi:10.1016/j.ajhg.2011.10.006

7. Daoud H, Tétreault M, Gibson W, et al. Mutations in POLR3A and POLR3B are a major cause of hypomyelinating leukodystrophies with or without dental abnormalities and/or hypogonadotropic hypogonadism. *J Med Genet*. 2013;50(3):194-197. doi:10.1136/jmedgenet-2012-101357

8. Watt KE, Macintosh J, Bernard G, Trainor PA. RNA Polymerases I and III in development and disease. *Semin Cell Dev Biol*. 2023;136:49-63. doi:10.1016/j.semcdb.2022.03.027

9. Perrier S, Gauquelin L, Fallet-Bianco C, et al. Expanding the phenotypic and molecular spectrum of RNA polymerase III–related leukodystrophy. *Neurol Genet*. 2020;6(3):e425. doi:10.1212/NXG.0000000000000425

10. Bonkowsky JL, Nelson C, Kingston JL, Filloux FM, Mundorff MB, Srivastava R. The burden of inherited leukodystrophies in children. *Neurology*. 2010;75(8):718-725. doi:10.1212/WNL.0b013e3181eee46b

11. Parikh S, Bernard G, Leventer RJ, et al. A clinical approach to the diagnosis of patients with leukodystrophies and genetic leukoencephelopathies. *Mol Genet Metab*. 2015;114(4):501-515. doi:10.1016/j.ymgme.2014.12.434

12. Adang LA, Sherbini O, Ball L, et al. Revised consensus statement on the preventive and symptomatic care of patients with leukodystrophies. *Mol Genet Metab*. 2017;122(1-2):18-32. doi:10.1016/j.ymgme.2017.08.006

13. Perrier S, Michell-Robinson MA, Bernard G. POLR3-Related Leukodystrophy: Exploring Potential Therapeutic Approaches. *Front Cell Neurosci*. 2021;14:631802. doi:10.3389/fncel.2020.631802

14. Krivit W. Allogeneic stem cell transplantation for the treatment of lysosomal and peroxisomal metabolic diseases. *Springer Semin Immunopathol*. 2004;26(1-2):119-132. doi:10.1007/s00281-004-0166-2

15. Krivit W, Peters C, Shapiro EG. Bone marrow transplantation as effective treatment of central nervous system disease in globoid cell leukodystrophy, metachromatic leukodystrophy, adrenoleukodystrophy, mannosidosis, fucosidosis, aspartylglucosaminuria, Hurler, Maroteaux-Lamy, and Sly syndromes, and Gaucher disease type III: *Curr Opin Neurol*. 1999;12(2):167-176. doi:10.1097/00019052-199904000-00007

16. van den Broek BTA, Page K, Paviglianiti A, et al. Early and late outcomes after cord blood transplantation for pediatric patients with inherited leukodystrophies. *Blood Adv*. 2018;2(1):49-60. doi:10.1182/bloodadvances.2017010645

17. Lata E, Choquet K, Sagliocco F, Brais B, Bernard G, Teichmann M. RNA Polymerase III Subunit Mutations in Genetic Diseases. *Front Mol Biosci*. 2021;8:696438. doi:10.3389/fmolb.2021.696438

18. Bernard G, Vanderver A. POLR3-Related Leukodystrophy. In: Adam MP, Ardinger HH, Pagon RA, et al., eds. *GeneReviews®*. University of Washington, Seattle; 2017. Accessed October 3, 2021. http://www.ncbi.nlm.nih.gov/books/NBK99167/

19. Wolf NI, Vanderver A, van Spaendonk RML, et al. Clinical spectrum of 4H leukodystrophy caused by POLR3A and POLR3B mutations. *Neurology*. 2014;83(21):1898-1905. doi:10.1212/WNL.0000000000001002

20. Gauquelin L, Cayami FK, Sztriha L, et al. Clinical spectrum of POLR3-related leukodystrophy caused by biallelic *POLR1C* pathogenic variants. *Neurol Genet*. 2019;5(6):e369. doi:10.1212/NXG.0000000000000369

21. Anderson RH, Francis KR. Modeling rare diseases with induced pluripotent stem cell technology. *Mol Cell Probes*. 2018;40:52-59. doi:10.1016/j.mcp.2018.01.001

22. Harting I, Al-Saady M, Krägeloh-Mann I, et al. POLR3A variants with striatal involvement and extrapyramidal movement disorder. *neurogenetics*. 2020;21(2):121-133. doi:10.1007/s10048-019-00602-4

23. Azmanov DN, Siira SJ, Chamova T, et al. Transcriptome-wide effects of a *POLR3A* gene mutation in patients with an unusual phenotype of striatal involvement. *Hum Mol Genet*. 2016;25(19):4302-4314. doi:10.1093/hmg/ddw263

24. Schiffmann R, van der Knaap MS. Invited Article: An MRI-based approach to the diagnosis of white matter disorders. *Neurology*. 2009;72(8):750-759. doi:10.1212/01.wnl.0000343049.00540.c8

25. van der Voorn JP, Pouwels PJW, Hart AAM, et al. Childhood White Matter Disorders: Quantitative MR Imaging and Spectroscopy. *Radiology*. 2006;241(2):510-517. doi:10.1148/radiol.2412051345

26. Knaap MS van der, Valk J, Barkhof F, Knaap MS van der. *Magnetic Resonance of Myelination and Myelin Disorders*. 3rd ed. Springer; 2005.

27. van der Knaap MS, Breiter SN, Naidu S, Hart AAM, Valk J. Defining and Categorizing Leukoencephalopathies of Unknown Origin: MR Imaging Approach. *Radiology*. 1999;213(1):121-133. doi:10.1148/radiology.213.1.r99se01121

28. Soderholm HE, Chapin AB, Bayrak-Toydemir P, Bonkowsky JL. Elevated Leukodystrophy Incidence Predicted From Genomics Databases. *Pediatr Neurol*. 2020;111:66-69. doi:10.1016/j.pediatrneurol.2020.06.005

29. Costello DJ, Eichler AF, Eichler FS. Leukodystrophies: Classification, Diagnosis, and Treatment. *The Neurologist*. 2009;15(6):319-328. doi:10.1097/NRL.0b013e3181b287c8

30. van der Knaap MS, Bugiani M. Leukodystrophies: a proposed classification system based on pathological changes and pathogenetic mechanisms. *Acta Neuropathol (Berl)*. 2017;134(3):351-382. doi:10.1007/s00401-017-1739-1

31. Vanderver A, Tonduti D, Schiffmann R, Schmidt JL, van der Knaap MS. Leukodystrophy Overview – RETIRED CHAPTER, FOR HISTORICAL REFERENCE ONLY. In: *GeneReviews® [Internet]*. Seattle (WA): University of Washington; 2014:1993-2017. https://www.ncbi.nlm.nih.gov/books/NBK184570/

32. Naidu S. Abstracts from the Fourth Symposium on Probing Disorders of the White Matter. *J Mol Neurosci*. 1999;12(3):185-192. doi:10.1385/JMN:12:3:185

33. Atrouni S, Darazé A, Tamraz J, Cassia A, Caillaud C, Mégarbané A. Leukodystrophy associated with oligodontia in a large inbred family: Fortuitous association or new entity?: Dento-Leukodystrophy Syndrome. *Am J Med Genet A*. 2003;118A(1):76-81. doi:10.1002/ajmg.a.10019

34. Chouery E, Delague V, Jalkh N, et al. A whole-genome scan in a large family with leukodystrophy and oligodontia reveals linkage to 10q22. *neurogenetics*. 2011;12(1):73-78. doi:10.1007/s10048-010-0256-3

35. Wolf N, Harting I, Innes A, et al. Ataxia, Delayed Dentition and Hypomyelination: A Novel Leukoencephalopathy. *Neuropediatrics*. 2007;38(2):64-70. doi:10.1055/s-2007-985137

36. Wolff A, Koch MJ, Benzinger S, et al. Rare dental peculiarities associated with the hypomyelinating leukoencephalopathy 4H syndrome/ADDH. *Pediatr Dent*. 2010;32(5):386-392.

37. Wolf NI, Harting I, Boltshauser E, et al. Leukoencephalopathy with ataxia, hypodontia, and hypomyelination. *Neurology*. 2005;64(8):1461-1464. doi:10.1212/01.WNL.0000158615.56071.E3

38. Timmons M, Tsokos M, Asab MA, et al. Peripheral and central hypomyelination with hypogonadotropic hypogonadism and hypodontia. *Neurology*. 2006;67(11):2066-2069. doi:10.1212/01.wnl.0000247666.28904.35

39. Vázquez-López M, Ruiz-Martín Y, de Castro-Castro P, Garzo-Fernández C, Martín-del Valle F, Márquez-de la Plata L. [Central hypomyelination, hypogonadotrophic hypogonadism and hypodontia: a new leukodystrophy]. *Rev Neurol*. 2008;47(4):204-208.

40. Sasaki M, Takanashi J ichi, Tada H, Sakuma H, Furushima W, Sato N. Diffuse cerebral hypomyelination with cerebellar atrophy and hypoplasia of the corpus callosum. *Brain Dev*. 2009;31(8):582-587. doi:10.1016/j.braindev.2008.09.003

41. Saitsu H, Osaka H, Sasaki M, et al. Mutations in POLR3A and POLR3B Encoding RNA Polymerase III Subunits Cause an Autosomal-Recessive Hypomyelinating Leukoencephalopathy. *Am J Hum Genet*. 2011;89(5):644-651. doi:10.1016/j.ajhg.2011.10.003

42. Bernard G, Thiffault I, Tetreault M, et al. Tremor–ataxia with central hypomyelination (TACH) leukodystrophy maps to chromosome 10q22.3–10q23.31. *neurogenetics*. 2010;11(4):457-464. doi:10.1007/s10048-010-0251-8

43. Bernard G, Chouery E, Putorti ML, et al. Mutations of POLR3A encoding a catalytic subunit of RNA polymerase Pol III cause a recessive hypomyelinating leukodystrophy. *Am J Hum Genet*. 2011;89(3):415-423. doi:10.1016/j.ajhg.2011.07.014

44. Tétreault M, Putorti ML, Thiffault I, et al. TACH Leukodystrophy: Locus Refinement to Chromosome 10q22.3-23.1. *Can J Neurol Sci J Can Sci Neurol*. 2012;39(1):122-123. doi:10.1017/S0317167100022174

45. Osterman B, Sylvain M, Chouinard S, Bernard G. Tremor-ataxia with central hypomyelination (TACH): Dystonia as a new clinical feature: Letters: new Observation. *Mov Disord*. 2012;27(14):1831-1832. doi:10.1002/mds.25270

46. Al Yazidi G, Tran LT, Guerrero K, et al. Dystonia in RNA Polymerase III-Related Leukodystrophy. *Mov Disord Clin Pract*. 2019;6(2):155-159. doi:10.1002/mdc3.12715

47. Pelletier F, Perrier S, Cayami FK, et al. Endocrine and Growth Abnormalities in 4H Leukodystrophy Caused by Variants in *POLR3A* , *POLR3B* , and *POLR1C*. *J Clin Endocrinol Metab*. 2021;106(2):e660-e674. doi:10.1210/clinem/dgaa700

48. Boycott KM, Dyment DA, Sawyer SL, Vanstone MR, Beaulieu CL. Identification of Genes for Childhood Heritable Diseases. *Annu Rev Med*. 2014;65(1):19-31. doi:10.1146/annurev-med-101712-122108

49. Srivastava S, Cohen JS, Vernon H, et al. Clinical whole exome sequencing in child neurology practice: WES in Child Neurology. *Ann Neurol*. 2014;76(4):473-483. doi:10.1002/ana.24251

50. Vanderver A, Simons C, Helman G, et al. Whole exome sequencing in patients with white matter abnormalities. *Ann Neurol*. 2016;79(6):1031-1037. doi:10.1002/ana.24650

51. Girbig M, Misiaszek AD, Vorländer MK, et al. *Cryo-EM Structures of Human RNA Polymerase III in Its Unbound and Transcribing States*. Molecular Biology; 2020. doi:10.1101/2020.06.29.177642

52. Ramsay EP, Abascal-Palacios G, Daiß JL, et al. Structure of human RNA polymerase III. *Nat Commun*. 2020;11(1):6409. doi:10.1038/s41467-020-20262-5

53. Djordjevic D, Pinard M, Gauthier MS, et al. De novo variants in POLR3B cause ataxia, spasticity, and demyelinating neuropathy. *Am J Hum Genet*. 2021;108(1):186-193. doi:10.1016/j.ajhg.2020.12.002

54. Richards MR, Plummer L, Chan YM, et al. Phenotypic spectrum of *POLR3B* mutations: isolated hypogonadotropic hypogonadism without neurological or dental anomalies. *J Med Genet*. 2017;54(1):19-25. doi:10.1136/jmedgenet-2016-104064

55. Ghoumid J, Petit F, Boute-Benejean O, et al. Cerebellar hypoplasia with endosteal sclerosis is a POLR3-related disorder. *Eur J Hum Genet*. 2017;25(8):1011-1014. doi:10.1038/ejhg.2017.73

56. Beauregard-Lacroix E, Salian S, Kim H, et al. A variant of neonatal progeroid syndrome, or Wiedemann–Rautenstrauch syndrome, is associated with a nonsense variant in POLR3GL. *Eur J Hum Genet*. 2020;28(4):461-468. doi:10.1038/s41431-019-0539-6

57. Paolacci S, Li Y, Agolini E, et al. Specific combinations of biallelic *POLR3A* variants cause Wiedemann-Rautenstrauch syndrome. *J Med Genet*. 2018;55(12):837-846. doi:10.1136/jmedgenet-2018-105528

58. Wambach JA, Wegner DJ, Patni N, et al. Bi-allelic POLR3A Loss-of-Function Variants Cause Autosomal-Recessive Wiedemann-Rautenstrauch Syndrome. *Am J Hum Genet*. 2018;103(6):968-975. doi:10.1016/j.ajhg.2018.10.010

59. Wu SW, Li L, Feng F, et al. Whole-exome sequencing reveals POLR3B variants associated with progeria-related Wiedemann-Rautenstrauch syndrome. *Ital J Pediatr*. 2021;47(1):160. doi:10.1186/s13052-021-01112-6

60. Jay AM, Conway RL, Thiffault I, et al. Neonatal progeriod syndrome associated with biallelic truncating variants in *POLR3A*. *Am J Med Genet A*. 2016;170(12):3343-3346. doi:10.1002/ajmg.a.37960

61. Perrier S, Gauquelin L, Wambach JA, Bernard G. Distinguishing severe phenotypes associated with pathogenic variants in *POLR3A*. *Am J Med Genet A*. 2022;188(2):708-712. doi:10.1002/ajmg.a.62553

62. Rautenstrauch T, Snigula F, Krieg T, Gay S, M□ller PK. Progeria: A cell culture study and clinical report of familial incidence. *Eur J Pediatr*. 1977;124(2):101-111. doi:10.1007/BF00477545

63. Wiedemann HR. An unidentified neonatal progeroid syndrome: Follow-up report. *Eur J Pediatr*. 1979;130(1):65-70. doi:10.1007/BF00441901

64. Terhal PA, Vlaar JM, Middelkamp S, et al. Biallelic variants in POLR3GL cause endosteal hyperostosis and oligodontia. *Eur J Hum Genet*. 2020;28(1):31-39. doi:10.1038/s41431-019-0427-0

65. Welting TJM, Mattijssen S, Peters FMA, et al. Cartilage–hair hypoplasia-associated mutations in the RNase MRP P3 domain affect RNA folding and ribonucleoprotein assembly. *Biochim Biophys Acta BBA - Mol Cell Res*. 2008;1783(3):455-466. doi:10.1016/j.bbamcr.2007.11.016

66. Martin AN, Li Y. RNase MRP RNA and human genetic diseases. *Cell Res*. 2007;17(3):219-226. doi:10.1038/sj.cr.7310120

67. Barba-Aliaga M, Alepuz P, Pérez-Ortín JE. Eukaryotic RNA Polymerases: The Many Ways to Transcribe a Gene. *Front Mol Biosci*. 2021;8:663209. doi:10.3389/fmolb.2021.663209

68. Dieci G, Fiorino G, Castelnuovo M, Teichmann M, Pagano A. The expanding RNA polymerase III transcriptome. *Trends Genet*. 2007;23(12):614-622. doi:10.1016/j.tig.2007.09.001

69. White RJ. Transcription by RNA polymerase III: more complex than we thought. *Nat Rev Genet*. 2011;12(7):459-463. doi:10.1038/nrg3001

70. Choquet K, Forget D, Meloche E, et al. Leukodystrophy-associated POLR3A mutations down-regulate the RNA polymerase III transcript and important regulatory RNA BC200. *J Biol Chem*. 2019;294(18):7445-7459. doi:10.1074/jbc.RA118.006271

71. Takahashi K, Yamanaka S. Induction of Pluripotent Stem Cells from Mouse Embryonic and Adult Fibroblast Cultures by Defined Factors. *Cell*. 2006;126(4):663-676. doi:10.1016/j.cell.2006.07.024

72. Freel BA, Sheets JN, Francis KR. iPSC modeling of rare pediatric disorders. *J Neurosci Methods*. 2020;332:108533. doi:10.1016/j.jneumeth.2019.108533

73. Steyer B, Cory E, Saha K. Developing precision medicine using scarless genome editing of human pluripotent stem cells. *Drug Discov Today Technol*. 2018;28:3-12. doi:10.1016/j.ddtec.2018.02.001

74. Bassett AR. Editing the genome of hiPSC with CRISPR/Cas9: disease models. *Mamm Genome Off J Int Mamm Genome Soc*. 2017;28(7-8):348-364. doi:10.1007/s00335-017-9684-9

75. Malankhanova T, Suldina L, Grigor'eva E, et al. A Human Induced Pluripotent Stem Cell-Derived Isogenic Model of Huntington's Disease Based on Neuronal Cells Has Several Relevant Phenotypic Abnormalities. *J Pers Med*. 2020;10(4):215. doi:10.3390/jpm10040215

76. O'Shea O, Steeg R, Chapman C, Mackintosh P, Stacey GN. Development and implementation of large-scale quality control for the European bank for induced Pluripotent Stem Cells. *Stem Cell Res*. 2020;45:101773. doi:10.1016/j.scr.2020.101773

77. Ran FA, Hsu PD, Wright J, Agarwala V, Scott DA, Zhang F. Genome engineering using the CRISPR-Cas9 system. *Nat Protoc*. 2013;8(11):2281-2308. doi:10.1038/nprot.2013.143

78. Lovinger DM. Communication networks in the brain: neurons, receptors, neurotransmitters, and alcohol. *Alcohol Res Health J Natl Inst Alcohol Abuse Alcohol*. 2008;31(3):196-214.

79. Kandel ER, ed. *Principles of Neural Science*. 5th ed. McGraw-Hill; 2013.

80. Zhao X, Moore DL. Neural stem cells: developmental mechanisms and disease modeling. *Cell Tissue Res*. 2018;371(1):1-6. doi:10.1007/s00441-017-2738-1

81. Xiuqing Chen, Cecilia Rocha, Martin Liognon, Huasheng Peng, Trisha Rao, Thomas M. Durcan. Induction of Dopaminergic or Cortical neuronal progenitors from iPSCs. Published online April 2020.

82. Ito K, Suda T. Metabolic requirements for the maintenance of self-renewing stem cells. *Nat Rev Mol Cell Biol*. 2014;15(4):243-256. doi:10.1038/nrm3772

83. Rafalski VA, Brunet A. Energy metabolism in adult neural stem cell fate. *Prog Neurobiol*. 2011;93(2):182-203. doi:10.1016/j.pneurobio.2010.10.007

84. Chambers SM, Fasano CA, Papapetrou EP, Tomishima M, Sadelain M, Studer L. Highly efficient neural conversion of human ES and iPS cells by dual inhibition of SMAD signaling. *Nat Biotechnol*. 2009;27(3):275-280. doi:10.1038/nbt.1529

85. Inman GJ, Nicolás FJ, Callahan JF, et al. SB-431542 Is a Potent and Specific Inhibitor of Transforming Growth Factor-β Superfamily Type I Activin Receptor-Like Kinase (ALK) Receptors ALK4, ALK5, and ALK7. *Mol Pharmacol*. 2002;62(1):65-74. doi:10.1124/mol.62.1.65

86. Neely MD, Litt MJ, Tidball AM, et al. DMH1, a highly selective small molecule BMP inhibitor promotes neurogenesis of hiPSCs: comparison of PAX6 and SOX1 expression during neural induction. *ACS Chem Neurosci*. 2012;3(6):482-491. doi:10.1021/cn300029t

87. BehindTheBench. PCR Primer Design Tips. Behind The Bench. Published September 25, 2019. https://www.thermofisher.com/blog/behindthebench/pcr-primer-design-tips/

88. Trevino AE, Zhang F. Genome Editing Using Cas9 Nickases. In: *Methods in Enzymology*. Vol 546. Elsevier; 2014:161-174. doi:10.1016/B978-0-12-801185-0.00008-8

89. Benchling. Published online 2022. https://benchling.com

90. Labun K, Montague TG, Krause M, Torres Cleuren YN, Tjeldnes H, Valen E. CHOPCHOP v3: expanding the CRISPR web toolbox beyond genome editing. *Nucleic Acids Res*. 2019;47(W1):W171-W174. doi:10.1093/nar/gkz365

91. Concordet JP, Haeussler M. CRISPOR: intuitive guide selection for CRISPR/Cas9 genome editing experiments and screens. *Nucleic Acids Res*. 2018;46(W1):W242-W245. doi:10.1093/nar/gky354

92. Ye H, Wang Q. Efficient Generation of Non-Integration and Feeder-Free Induced Pluripotent Stem Cells from Human Peripheral Blood Cells by Sendai Virus. *Cell Physiol Biochem*. 2018;50(4):1318-1331. doi:10.1159/000494589

93. Chen X, Cecilia Rocha, Trisha Rao. iPSC Culture. Published online 2020.

94. Castro-Viñuelas R, Sanjurjo-Rodríguez C, Piñeiro-Ramil M, et al. Tips and tricks for successfully culturing and adapting human induced pluripotent stem cells. *Mol Ther - Methods Clin Dev*. 2021;23:569-581. doi:10.1016/j.omtm.2021.10.013

95. Chatterjee P, Cheung Y, Liew C. Transfecting and Nucleofecting Human Induced Pluripotent Stem Cells. *J Vis Exp*. 2011;(56):3110. doi:10.3791/3110

96. Hindson BJ, Ness KD, Masquelier DA, et al. High-Throughput Droplet Digital PCR System for Absolute Quantitation of DNA Copy Number. *Anal Chem*. 2011;83(22):8604-8610. doi:10.1021/ac202028g

97. Swindell SR, Plasterer TN. SEQMAN. Contig assembly. *Methods Mol Biol Clifton NJ*. 1997;70:75-89.

98. StemCell Technologies. hPSC Genetic Analysis Kit. Published online 2019.

99. Zhang X, Huang CT, Chen J, et al. Pax6 Is a Human Neuroectoderm Cell Fate Determinant. *Cell Stem Cell*. 2010;7(1). doi:10.1016/j.stem.2010.04.017

100. Lendahl U, Zimmerman LB, McKay RDG. CNS stem cells express a new class of intermediate filament protein. *Cell*. 1990;60(4):585-595. doi:10.1016/0092-8674(90)90662-X

101. Ikeda H, Osakada F, Watanabe K, et al. Generation of Rx $^{+}$ /Pax6 $^{+}$ neural retinal precursors from embryonic stem cells. *Proc Natl Acad Sci*. 2005;102(32). doi:10.1073/pnas.0500010102

102. Su Z, Zhang Y, Liao B, et al. Antagonism between the transcription factors NANOG and OTX2 specifies rostral or caudal cell fate during neural patterning transition. *J Biol Chem*. 2018;293(12):4445-4455. doi:10.1074/jbc.M117.815449

103. Suter DM, Tirefort D, Julien S, Krause KH. A Sox1 to Pax6 Switch Drives Neuroectoderm to Radial Glia Progression During Differentiation of Mouse Embryonic Stem Cells. *Stem Cells*. 2009;27(1). doi:10.1634/stemcells.2008-0319

104. Venere M, Han YG, Bell R, Song JS, Alvarez-Buylla A, Blelloch R. Sox1 marks an activated neural stem/progenitor cell in the hippocampus. *Development*. 2012;139(21). doi:10.1242/dev.081133

105. Sun W, Cornwell A, Li J, et al. SOX9 Is an Astrocyte-Specific Nuclear Marker in the Adult Brain Outside the Neurogenic Regions. *J Neurosci*. 2017;37(17). doi:10.1523/JNEUROSCI.3199-16.2017

106. Nicholson DW, Ali A, Thornberry NA, et al. Identification and inhibition of the ICE/CED-3 protease necessary for mammalian apoptosis. *Nature*. 1995;376(6535):37-43. doi:10.1038/376037a0

107. Li LT, Jiang G, Chen Q, Zheng JN. Ki67 is a promising molecular target in the diagnosis of cancer (Review). *Mol Med Rep*. 2015;11(3):1566-1572. doi:10.3892/mmr.2014.2914

108. Deneault E, Micheal Nicouleau, Thomas M. Durcan. CRISPR-mediated introduction of single nucleotide changes in iPSCs. Published online 2020.

109. Na J, Baker D, Zhang J, Andrews PW, Barbaric I. Aneuploidy in pluripotent stem cells and implications for cancerous transformation. *Protein Cell*. 2014;5(8):569-579. doi:10.1007/s13238-014-0073-9

110. Avery S, Hirst AJ, Baker D, et al. BCL-XL Mediates the Strong Selective Advantage of a 20q11.21 Amplification Commonly Found in Human Embryonic Stem Cell Cultures. *Stem Cell Rep*. 2013;1(5):379-386. doi:10.1016/j.stemcr.2013.10.005

111. Nguyen HT, Geens M, Mertzanidou A, et al. Gain of 20q11.21 in human embryonic stem cells improves cell survival by increased expression of Bcl-xL. *MHR Basic Sci Reprod Med*. 2014;20(2):168-177. doi:10.1093/molehr/gat077

112. Oda E, Ohki R, Murasawa H, et al. Noxa, a BH3-Only Member of the Bcl-2 Family and Candidate Mediator of p53-Induced Apoptosis. *Science*. 2000;288(5468):1053-1058. doi:10.1126/science.288.5468.1053

113. Booy EP, McRae EK, Koul A, Lin F, McKenna SA. The long non-coding RNA BC200 (BCYRN1) is critical for cancer cell survival and proliferation. *Mol Cancer*. 2017;16(1):109. doi:10.1186/s12943-017-0679-7

114. Shin H, Lee J, Kim Y, et al. Knockdown of BC200 RNA expression reduces cell migration and invasion by destabilizing mRNA for calcium-binding protein S100A11. *RNA Biol*. 2017;14(10):1418-1430. doi:10.1080/15476286.2017.1297913

115. Singh R, Gupta SC, Peng WX, et al. Regulation of alternative splicing of Bcl-x by BC200 contributes to breast cancer pathogenesis. *Cell Death Dis*. 2016;7(6):e2262-e2262. doi:10.1038/cddis.2016.168

116. Shin H, Lee J, Kim Y, Jang S, Ohn T, Lee Y. Identifying the cellular location of brain cytoplasmic 200 RNA using an RNA-recognizing antibody. *BMB Rep*. 2017;50(6):318-322. doi:10.5483/BMBRep.2017.50.6.217

117. Báez-Becerra CT, Valencia-Rincón E, Velásquez-Méndez K, et al. Nucleolar disruption, activation of P53 and premature senescence in POLR3A-mutated Wiedemann-Rautenstrauch syndrome fibroblasts. *Mech Ageing Dev*. 2020;192:111360. doi:10.1016/j.mad.2020.111360

118. Shimojima K, Shimada S, Tamasaki A, et al. Novel compound heterozygous mutations of POLR3A revealed by whole-exome sequencing in a patient with hypomyelination. *Brain Dev*. 2014;36(4):315-321. doi:10.1016/j.braindev.2013.04.011